

NASA Technical Memorandum 4699

Fatigue Parameter Estimation Methodology for Power and Paris Crack Growth Laws in Monolithic Ceramic Materials

Bernard Gross, Lynn M. Powers,
Osama M. Jadaan, and Lesley A. Janosik

MARCH 1996



National Aeronautics and
Space Administration

Fatigue Parameter Estimation Methodology for Power and Paris Crack Growth Laws in Monolithic Ceramic Materials

Bernard Gross
Lewis Research Center
Cleveland, Ohio

Lynn M. Powers
Cleveland State University
Cleveland, Ohio

Osama M. Jadaan
University of Wisconsin-Platteville
Platteville, Wisconsin

Lesley A. Janosik
Lewis Research Center
Cleveland, Ohio



National Aeronautics and
Space Administration

Office of Management

Scientific and Technical
Information Program

1996

Contents

Summary	1
Introduction	1
Symbols	2
Theoretical Development	3
Power Law	3
Analysis	3
Parameter estimation	6
Method I—Least-squares best fit using median values	6
Method II—Maximum likelihood estimation using median values	7
Method III—Least-squares best fit using all fatigue rupture data	7
Method IV—Maximum likelihood estimation using all fatigue rupture data	7
Method V—Least-squares best fit to evaluate unsubscripted B	7
Method VI—Median deviation	7
Dynamic fatigue	7
Paris Law	8
Analysis	9
Parameter estimation	10
Method I—Least-squares best fit using median values	10
Method II—Maximum likelihood estimation using median values	10
Method III—Least-squares best fit using all fatigue rupture data	10
Method IV—Maximum likelihood estimation using all fatigue rupture data	11
Method V—Least-squares best fit to evaluate unsubscripted B	11
Method VI—Median deviation	11
Walker Law	11
Analysis	11
Parameter estimation	13
Method I—Least-squares best-fit regression plane using median values	13
Method II—Least-squares best-fit regression plane using all data	13
Method III—Least-squares best-fit regression plane to evaluate unsubscripted B	13
Method IV—Maximum likelihood estimation using all data	13
Experimental Applications	13
Soda Lime Glass	14
Inert data analysis	14
Dynamic fatigue data analysis	15
Sintered Alpha Silicon Carbide	18
Inert data analysis	18
Dynamic fatigue data analysis	19
Conclusions	23
References	24

Fatigue Parameter Estimation Methodology for Power and Paris Crack Growth Laws in Monolithic Ceramic Materials

Bernard Gross*

National Aeronautics and Space Administration
Lewis Research Center
Cleveland, Ohio 44135

Lynn M. Powers†

Cleveland State University
Cleveland, Ohio 44115

Osama M. Jadaan‡

University of Wisconsin-Platteville
Platteville, Wisconsin 53818

and

Lesley A. Janosik

National Aeronautics and Space Administration
Lewis Research Center
Cleveland, Ohio 44135

Summary

Material parameters (inert and fatigue) are obtained from naturally flawed specimens. If the inert strength parameters characterizing the two-parameter Weibull cumulative distribution function are known, the fatigue parameters for the power, Paris, and Walker subcritical crack growth equations can be obtained from the appropriate rupture data of standard uniaxial test specimens loaded in static, dynamic, or cyclic fatigue. Equations are developed for fatigue parameter analysis using the least-squares best-fit and/or the maximum likelihood estimation method. When the inert parameters are unknown and only subcritical crack growth rupture data are available, the material parameters defining the specimen's cumulative distribution function are obtained via the median deviation method. Example problems are included.

Introduction

The objective of this report is to introduce a number of techniques to obtain the necessary material parameters for a time-dependent reliability analysis of monolithic structural ceramic components. These parameters (inert and fatigue) are evaluated

from fast-fracture and time-dependent stress rupture data of uniaxially loaded test specimens. Ideally, the data are obtained under conditions representative of the service environment.

Static, dynamic, and/or cyclic fatigue loading result in a phenomenon called subcritical crack growth (SCG). Static fatigue is defined as the application of a constant load over a period of time. Dynamic fatigue is the application of a constant stress rate over a period of time, and cyclic fatigue is the repeated application of a loading sequence. Under tensile loading, SCG initiates at existing flaws and continues until a flaw reaches a critical length, causing catastrophic failure. Various laws such as the power (ref. 1), Paris (ref. 2), and Walker (ref. 3) are used to describe SCG. These laws are usually obtained from mode I laboratory tests of an introduced crack of known geometry. An uncertainty is involved in relating these results to a body containing a random distribution and orientation of inherent flaws of varied geometry and their interaction under mixed-mode loading. Parameters of the various SCG flaws, derived from naturally flawed test specimens, tend to compensate for these uncertainties, leading to better agreement between prediction and experimental data.

For the power, Paris, and Walker laws, analytical methods are derived to estimate the material parameters for volume flaws. Analogous equations are obtained for the condition

*Distinguished Research Associate

†NASA Resident Research Associate at Lewis Research Center.

‡Summer Faculty Fellow at Lewis Research Center.

where surface flaws are dominant. Using the least-squares best-fit (LSBF), the median deviation (MD), and the maximum likelihood estimation (MLE) methods, equations are developed for material parameter estimation. The Theoretical Development section consists of a brief development of background equations for each of the SCG laws, followed by descriptive techniques for estimating the parameters.

Two example problems are given in the section Experimental Applications. Data from soda lime glass ring-on-ring and sintered alpha silicon carbide (SASC) C-ring and O-ring specimens (refs. 4 and 5 and Nemeth, N.N. et al.: CARES/LIFE Ceramic Analysis and Reliability Evaluation of Structures Life Prediction Program. NASA Lewis Research Center, unpublished data, 1993.) are used to illustrate the application of some of the methods derived herein.

Symbols

A	material fatigue parameter (power law)	P_f	probability of failure
A_e	effective area (fast fracture)	Q	Walker law fatigue parameter
A_{ef}	effective area (subcritical crack growth)	R	ratio of minimum to maximum effective stress in a loading cycle
A_o	material fatigue parameter (Paris law)	R_i	inner specimen radius
a	crack half-length	R_o	outer specimen radius
B	fatigue constant	R_s	diagonal half-length (fig. 1)
C	function dependent on model and value of probability of failure	r	ring-on-ring radial location
exp	Naperian base	S	variate in equation (70)
g	g-factor for cyclic load conversion (eq. (8))	T	time interval for one load cycle
H	step function	t	time
h	ring-on-ring specimen thickness	V	volume
K	stress intensity factor	V_e	effective volume (fast fracture)
ℓn	natural logarithm	V_{ef}	effective volume (subcritical crack growth)
m	Weibull modulus	x,y,z	Cartesian coordinate locations
N	fatigue exponent	Y	geometric crack shape factor
n	number of cycles	Z	parameter associated with MLE (eq. (70))
P	applied load	Γ	gamma function
		ν	Poisson's ratio
		σ	stress
		$\dot{\sigma}$	stress rate
		σ_o	Weibull scale factor
		σ_θ	characteristic strength
		Ψ	represents location (x,y,z) of equivalent stress within the body
		Ψ_0	represents location (x_0,y_0,z_0) of maximum tensile principal stress within the body
		Subscripts:	
		c	cyclic

f	fracture
I	mode I
I_c	mode I critical
I_{eq}	mode I equivalent
i, j	subscripts denote i^{th} (j^{th}) datum in data set
ℓ	step function time switch
max	maximum
min	minimum
r	radial
s	surface
T	transformed
tan	tangential
u	uniaxial
v	volume
w	Weibull
0.5	denotes median value
1	maximum principal

Theoretical Development

The lifetime reliability of a structural ceramic component depends on the material's inert parameters (m , σ_o) and the fatigue parameters (N , B) which characterize subcritical crack growth. Material parameter estimation methods are developed for the power, Paris, and Walker equations. The power law expresses the crack growth increment per unit time, whereas the Paris and Walker models express the crack growth increment per cycle. The analytical relationships in this section have been derived for volume flaws; analogous relations are obtained for the case where surface flaws dominate.

Power Law

Analysis.—Dynamic or cyclic fatigue stress in conjunction with the power law is transformed into an equivalent static stress through the use of g-factors. Implicit in this conversion is the assumption that over the same time interval the equivalent

static stress will cause the same crack growth as the dynamic or cyclic stress (ref. 6).

For the uniaxial case, the crack growth is expressed as $da/dt = AK_I^N$. For volume flaws the general case is

$$\frac{da(\Psi, t)}{dt} = A K_{I_{eq}}^{N_v}(\Psi, t) \quad (1)$$

where a is the half-crack length; Ψ is the location point; t is the time; A is the material fatigue parameter; $K_{I_{eq}}$ is the mode I equivalent stress intensity factor; and N_v is the volume fatigue exponent.

The term $K_{I_{eq}}$ is defined as

$$K_{I_{eq}}(\Psi, t) = \sigma_{I_{eq}}(\Psi, t) Y \sqrt{a(\Psi, t)} \quad (2)$$

where $\sigma_{I_{eq}}$ is the mode I equivalent stress and Y is the geometric crack shape parameter.

Rearranging equation (2) and solving for the crack half-length yields

$$a(\Psi, t) = \left(\frac{K_{I_c}}{Y} \right)^2 \sigma_{I_{eq}, t}^{-2}(\Psi, t) \quad (3)$$

where K_{I_c} is the mode I critical stress intensity factor and $\sigma_{I_{eq}, t}$ is the equivalent stress at time t . From equations (1) to (3), the equivalent stress distribution at a failure time t_f is transformed to its inert effective stress distribution $\sigma_{I_{eq}, 0}(\Psi)$ at time $t = 0$ (refs. 7 and 8):

$$\sigma_{I_{eq}, 0}(\Psi) = \left[\frac{\int_0^{t_f} \sigma_{I_{eq}}^{N_v}(\Psi, t) dt}{B} + \sigma_{I_{eq}}^{N_v-2}(\Psi, t_f) \right]^{1/(N_v-2)} \quad (4)$$

where $\sigma_{I_{eq}, 0}(\Psi, t)$ is the same as $\sigma_{I_{eq}}(\Psi, t)$ and the fatigue constant B is

$$B = \frac{2}{A Y^2 K_{I_c}^{N_v-2} (N_v - 2)} \quad (5)$$

When the initial flaw size is much smaller than the flaw size at failure and the fatigue parameter N_v is large, as is the case for ceramics, equation (4) reduces to

$$\sigma_{Ieq,0}(\Psi) = \left[\frac{\int_0^{t_f} \sigma_{Ieq}^{N_v}(\Psi, t) dt}{B} \right]^{1/(N_v-2)} \quad (6)$$

Next follows an analysis of static and cyclic fatigue. Satisfying the assumption that the equivalent static stress distribution $\sigma_{Ieq}(\Psi)$ produces the same amount of crack growth as the periodic cyclic stress distribution over one cycle's time interval T results in

$$\sigma_{Ieq}(\Psi) = g(\Psi)^{1/N_v} \sigma_{Ieqc_{max}}(\Psi) \quad (7)$$

where the g -factor is defined as

$$g(\Psi) = \left\{ \frac{\int_0^T \left[\frac{\sigma_{Ieqc}(\Psi, t)}{\sigma_{Ieqc_{max}}(\Psi)} \right]^{N_v} dt}{T} \right\} \quad (8)$$

The g -factor for static and dynamic fatigue are available in closed form. Numerical integration is required for most load conditions. A summary of g -factors for various loading functions is given in table I.

The fatigue parameters N and B are calculated from rupture test data obtained from uniaxially loaded specimens. For a given applied constant static stress level j , $[\sigma_{Ieqc_{max}}(\Psi_0)]_j = \sigma_{fj}(\Psi_0)$ and the time to failure of the i^{th} specimen is t_{fji} . For static or cyclic fatigue, the g -factor will appear in the computation of the maximum equivalent static stress at location Ψ_0 . The data $(\sigma_{fj}(\Psi_0), t_{fji})$ are ranked for each stress level j , where j varies from 1 to q , and i varies from 1 to p . For the i^{th} specimen of rank r , using Benard's formula (ref. 9), $P_{fji} = (r - 0.3)/(p + 0.4)$.

For the specimen uniaxial Weibull model, the characteristic strength $\sigma_{\theta v}$ is dependent on the specimen geometry. The probability of failure P_{fji} is expressed as

$$P_{fji}(t_{fji}) = 1 - \exp \left\{ - \left[\frac{\sigma_{1ji,0}(\Psi_0)}{\sigma_{\theta v}} \right]^{m_v} \right\} \quad (9)$$

where m_v is the Weibull modulus, and Ψ_0 is the location of the maximum principal stress at failure.

Hence,

$$\begin{aligned} \sigma_{1ji,0}(\Psi_0) &= \left[\frac{\sigma_{1j}^{N_v}(\Psi_0) g(\Psi_0) t_{fji}}{B_{uv}} \right]^{1/(N_v-2)} \\ &= \left[\frac{\sigma_{fj}^{N_v}(\Psi_0) g(\Psi_0) t_{fji}}{B_{uv}} \right]^{1/(N_v-2)} \end{aligned} \quad (10)$$

Subscript 1 denotes the maximum principal tensile stress at fracture. Equation (10) with σ_{fj} equal to σ_{1j} represents the transformation of the maximum principal static stress $\sigma_{fj}(\Psi_0) g^{1/N_v}(\Psi_0)$ at t_{fji} to the inert stress $\sigma_{1ji,0}(\Psi_0)$ at $t = 0$.

For the uniaxial Weibull model, the scale factor σ_{ov} is a material property and the probability of failure is expressed as

$$P_{fji}(t_{fji}) = 1 - \exp \left\{ - \left[\left(\frac{1}{\sigma_{ov}} \right)^{m_v} \int_V \sigma_{1ji,0}^{m_v}(\Psi) dV \right] \right\} \quad (11)$$

with the integration over the volume V and

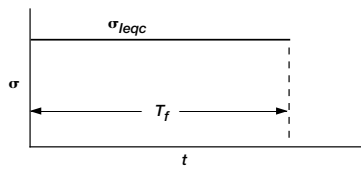
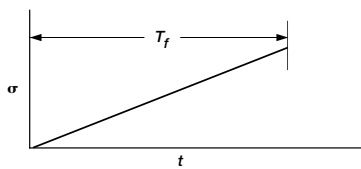
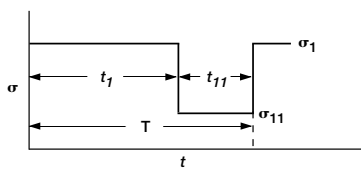
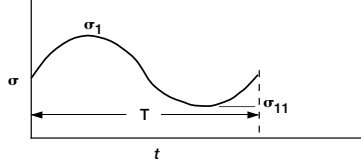
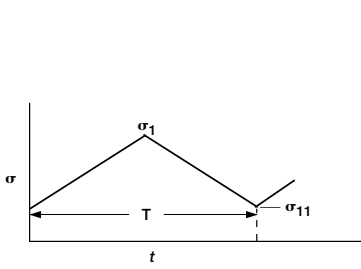
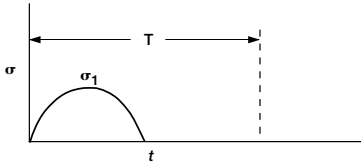
$$\begin{aligned} \sigma_{1ji,0}(\Psi) &= \left[\frac{\sigma_{1j}^{N_v}(\Psi) g(\Psi) t_{fji}}{B_{wv}} \right]^{1/(N_v-2)} \\ &= \left[\frac{\sigma_{fj}^{N_v}(\Psi) g(\Psi) t_{fji}}{B_{wv}} \right]^{1/(N_v-2)} \end{aligned} \quad (12)$$

Equation (12) represents the transformation of the equivalent static stress distribution at time t_{fji} to an inert stress distribution $\sigma_{1ji,0}(\Psi)$ at $t = 0$.

For the compatibility of failure probabilities, a basic requirement is that all models produce the same probability of failure for a uniaxial stress state as that obtained for the specimen uniaxial Weibull model. To satisfy this requirement, the value of N_v remains invariant whereas the fatigue parameter B will depend on the probability-of-failure model. All failure model dependent fatigue parameters (such as B_{uv} , the specimen uniaxial Weibull model) are directly proportional to B which is given by equation (5). For large values of N_v , all failure model dependent fatigue parameters approach a common value.

TABLE I.—g-FACTORS FOR VARIOUS LOADING FUNCTIONS^a

[$H(t, t_f) = 1$ for $t \geq t_f$; $H(t, t_f) = 0$ for $t < t_f$; ^b $\sigma_{11} \geq 0$.]

Loading function, $\sigma_{ieqc}(t)$	g-Factor, $g = \frac{1}{T} \int_0^T \left(\frac{\sigma_{ieqc}(t)}{\sigma_{ieqc_{max}}} \right)^N dt$	Waveform
Static fatigue $\sigma_{ieqc} = \text{Constant}$	1	
Dynamic fatigue $\sigma_{ieqc}(t) = \dot{\sigma} t$	$\frac{1}{N+1}$	
Cyclic square wave $\sigma_{ieqc}(t) = \sigma_1[H(t, 0) - H(t, t_1)] + \sigma_{11}[H(t, t_1) - H(t, T)]$	$\frac{t_1 + \left(\frac{\sigma_{11}}{\sigma_1}\right)^{N+1} t_{11}}{t_1 + t_{11}}$	
Sine wave $\sigma_{ieqc}(t) = \left(\frac{\sigma_1 - \sigma_{11}}{2}\right) \sin\left(\frac{2\pi t}{T}\right) + \left(\frac{\sigma_1 + \sigma_{11}}{2}\right)$	$\frac{1}{T} \int_0^T \left[\frac{\sigma_1 + \sigma_{11} + (\sigma_1 - \sigma_{11}) \sin\left(\frac{2\pi t}{T}\right)}{2\sigma_1} \right]^N dt$	
Cyclic sawtooth wave $\sigma_{ieqc}(t) = \left[\frac{2(\sigma_1 - \sigma_{11})t}{T} + \sigma_{11} \right] \times \left[H\left(t, \frac{T}{2}\right) - H\left(t, 0\right) \right] + \left[\frac{-2(\sigma_1 - \sigma_{11})t}{T} + 2\sigma_1 - \sigma_{11} \right] \times \left[H\left(t, \frac{T}{2}\right) - H\left(t, T\right) \right]$	$\frac{\sigma_1 - \sigma_{11} \left(\frac{\sigma_{11}}{\sigma_1}\right)^{N+1}}{(N+1)(\sigma_1 - \sigma_{11})}$	
Positive half-pulse of sine wave $\sigma_{ieqc}(t) = \left[\sigma_1 \sin\left(\frac{2\pi t}{T}\right) \right] \left[H\left(t, 0\right) - H\left(t, \frac{T}{2}\right) \right]$	$\frac{\Gamma\left(\frac{N+1}{2}\right)}{\sqrt{\pi} N \Gamma\left(\frac{N}{2}\right)}$	

^aNemeth, N.N. et al.: CARES/LIFE Ceramic Analysis and Reliability Evaluation of Structures Life Prediction Program, NASA Lewis Research Center, unpublished data, 1993.

^bWhen $\sigma_{11} < 0$, the value of the g -factor is generally obtained numerically by integrating over the time interval where $\sigma_{ieqc}(t) \geq 0$. The following simple example illustrates how this case is treated. Given a sawtooth cyclic wave defined by (t, σ) over time interval T as $(0, \sigma_1)$, $(T/2, \sigma_1)$, and (T, σ_{11}) with $R = \sigma_1/\sigma_{11}$

$$= -1/3. \text{ The interval where } \sigma_{ieqc}(t) \geq 0 \text{ is } \left[\frac{1}{1 + |\sigma_{11}/\sigma_1|} \right] T = 3T/4. \text{ Hence, } g = 2T \int_{T/8}^{T/2} \left\{ \left[\frac{2(\sigma_1 - \sigma_{11})t/T + \sigma_{11}}{\sigma_1} \right]^N dt \right.$$

$$= 2T \int_{T/8}^{T/2} \left\{ [2(1-R)t/T + R]^N dt \right. \text{ Thus, the resulting } g\text{-factor is } g = 3/[4(N+1)].$$

Equating the risk of rupture of the specimen uniaxial Weibull model to that of the uniaxial Weibull model results in

$$\left(\frac{B_{wv}}{B_{uv}}\right)^{m_v/(N_v-2)} = \left[\left(\frac{\sigma_{ov}}{\sigma_{\theta v}}\right)^{-m_v} \int_v \left(\frac{\sigma_{ff}(\Psi)}{\sigma_{ff}(\Psi_0)}\right)^{(m_v N_v)/(N_v-2)} dV = \frac{V_{ef}}{V_e} \right]$$

where V_e is the effective volume for no subcritical crack growth, and V_{ef} is the effective volume when subcritical crack growth occurs:

$$V_e = \left(\frac{\sigma_{ov}}{\sigma_{\theta v}}\right)^{m_v}$$

and

$$V_{ef} = \int_v \left(\frac{\sigma_{ff}(\Psi)}{\sigma_{ff}(\Psi_0)}\right)^{(m_v N_v)/(N_v-2)} dV$$

Using the above equations to eliminate $\sigma_{\theta v}$ and B_{uv} from the specimen uniaxial Weibull model yields

$$P_{fji}(t_{fji}) = 1 - \exp\left\{-\left[\frac{\sigma_{ff}^{N_v}(\Psi_0)g(\Psi_0)t_{fji}V_{ef}^{1/\tilde{m}_v}}{B_{wv}\sigma_{ov}^{N_v-2}}\right]^{\tilde{m}_v}\right\} \quad (13)$$

where $\tilde{m}_v = m_v/(N_v - 2)$. Thus,

$$t_{fji} = \left\{ \frac{B_{wv}\sigma_{ov}^{N_v-2}}{\left[\frac{V_{ef}}{\ln(1-P_{fji})^{-1}}\right]^{1/\tilde{m}_v} g(\Psi_0)} \right\}^{-1/\tilde{m}_v} \sigma_{ff}^{-N_v}(\Psi_0) = C_{ji}\sigma_{ff}^{-N_v}(\Psi_0) \quad (14)$$

where C_{ji} varies with the probability of failure P_{fji} . Taking the natural logarithm of equation (13) and manipulating it algebraically yields

$$\begin{aligned} \ln t_{fji} + \frac{2\ln\left[\ln(1-P_{fji})^{-1}\right]}{m_v} \\ = N_v \left\{ \frac{\ln\left[\ln(1-P_{fji})^{-1}\right]}{m_v} - \ln \sigma_{ff}(\Psi_0) \right\} - \ln \left[\frac{g(\Psi_0)V_{ef}^{1/\tilde{m}_v}}{B_{wv}\sigma_{ov}^{N_v-2}} \right] \end{aligned} \quad (15)$$

This equation is the basis for a least-squares best-fit evaluation of the fatigue parameters N_v and B_{wv} using all the available rupture data. If the same risk of rupture is maintained, from equation (13), all fatigue rupture data $(\sigma_{ff}(\Psi_0), t_{fji})$ can be transformed to an equivalent data set $(\sigma_T(\Psi_0), t_{Tji})$ for a given value of N_v :

$$t_{Tji} = \left[\frac{\sigma_{ff}(\Psi_0)}{\sigma_T(\Psi_0)}\right]^{N_v} t_{fji} \quad (16)$$

$$\sigma_T(\Psi_0) = \min[\sigma_{ff}(\Psi_0)]$$

Subscript T denotes the transformed data. The probability of failure for this case is

$$P_{fji}(t_{Tji}) = 1 - \exp\left\{-\left[\frac{t_{Tji}}{\left[\frac{B_{wv}\sigma_{ov}^{N_v-2}}{\sigma_T^{N_v}(\Psi_0)g(\Psi_0)V_{ef}^{1/\tilde{m}_v}}\right]^{1/\tilde{m}_v}}\right]^{\tilde{m}_v}\right\} \quad (17)$$

Parameter estimation.—The following are techniques which may be used to determine the parameters for static and cyclic and then for dynamic fatigue using the power law formulation just described.

Method I—Least-squares best fit using median values: The inert material parameters m_v and σ_{ov} are known. For the median values, and taking the natural logarithm, equation (14) yields

$$\ln(t_{fji})_{0.5} = -N_v \ln[\sigma_{ff}(\Psi_0)]_{0.5} + \ln(C_{ji})_{0.5}$$

where subscript 0.5, denotes the median value. Since $P_{fji} = 0.5$, intercept $(C_{ji})_{0.5}$ is a constant. Substituting the set of median

values $(\sigma_{ff}(\Psi_0), t_{fji})_{0.5}$ into the above equation permits solving for slope N_v and intercept $(C_{ji})_{0.5}$. From the known value of N_v , $g(\Psi_0)$ and V_{ef} can be computed. From the value of the intercept, B_{wv} is obtained.

Method II—Maximum likelihood estimation using median values: The inert material parameters are known. Based on the least-squares best-fit result for N_v as a starting value (N_{assumed}), the median values $(\sigma_{ff}(\Psi_0), t_{fji})_{0.5}$ are transformed via equation (16) to the data set $(\sigma_T(\Psi_0), t_{Tji})_{0.5}$. The maximum likelihood estimation method is applied to equation (17) with t_{Tji} as the variate to obtain the value \tilde{m}_v . From this value, N_v computed can be determined and compared with N_{assumed} . When both values are within some specified tolerance, the solution is obtained. If not, the two values are averaged and the process is repeated. After convergence, the g -factor, V_{ef} and then B_{wv} are evaluated.

Method III—Least-squares best fit using all fatigue rupture data: The inert material parameters are known. The data are ranked for each value of $\sigma_{ff}(\Psi_0)$ in accordance with the magnitude of t_{fji} to obtain the data set $(\sigma_{ff}(\Psi_0), t_{fji}, P_{fji})$. Substituting these values into equation (15) permits solving for N_v and the intercept. The value of N_v is used to evaluate the g -factor and V_{ef} , and the intercept is used to solve for B_{wv} .

Method IV—Maximum likelihood estimation using all fatigue rupture data: The inert material parameters are known. A value of N_v is assumed based on the least-squares best-fit regression analysis. All the data are transformed via equation (16). The maximum likelihood estimation method is applied to equation (17) with t_{Tji} as the variate to solve for \tilde{m}_v . The value of N_v is computed and compared with the assumed value. These two values are averaged and the process is repeated until the assumed value is within a specified tolerance of the computed value. When this tolerance is achieved, $g(\Psi_0)$, V_{ef} , and B_{wv} are evaluated.

Method V—Least-squares best fit to evaluate unsubscripted B : The value of B in equation (6) is not model dependent and can be obtained by using both inert and fatigue rupture data. Equation (6) for static and cyclic fatigue reduces to

$$\sigma_{1ji,0}^{N_v-2}(\Psi_0) = \frac{\sigma_{ff}^{N_v}(\Psi_0)g(\Psi_0)t_{fji}}{B} \quad (18)$$

where $\sigma_{1ji,0}(\Psi_0)$ is the inert strength (maximum principal stress at fracture) obtained from the rupture data associated with $(\sigma_{ff}(\Psi_0), t_{fji})$ by equivalence of rank (P_{fji}). From equation (18) after some algebraic manipulation,

$$\begin{aligned} \ln t_{fji} + 2 \ln \sigma_{1ji,0}(\Psi_0) &= N_v \left[\ln \sigma_{1ji,0}(\Psi_0) - \ln \sigma_{ff}(\Psi_0) \right] \\ &+ \ln \left[\frac{B}{g(\Psi_0)} \right] \quad (19) \end{aligned}$$

For the set of data $(\sigma_{ff}(\Psi_0), t_{fji}, P_{fji})$, the equivalence of failure probability allows determining $(\sigma_{1ji,0}, P_{fji})$. These values are substituted in the above equation to solve for N_v and the intercept. The g -factor is evaluated using the value of N_v , and B is obtained from the intercept. A one-to-one correspondence of the inert data to the fatigue data is assumed.

Method VI—Median deviation: The median deviation (ref. 10) method is a measure of the spread of the data about the median value. This approach is used when the inert parameters are unknown and only time-dependent fatigue rupture data are available. From the minimization of the median deviation, the material parameters m_v , N_v , and $B_{wv} \sigma_{ov}^{N_v-2}$ are evaluated. For an assumed value of N_v , the data $(\sigma_{ff}(\Psi_0), t_{fji})$ are transformed via equation (16) into $(\sigma_T(\Psi_0), t_{Tji})$. From the transformed data, the median deviation for the total number of data points qp is

$$MD = \frac{1}{pq} \sum_{j=1}^q \sum_{i=1}^p \left| \ln t_{Tji} - \ln t_{T0.5} \right| \frac{1}{\tilde{m}_v pq} \sum_{j=1}^q \sum_{i=1}^p \left| \ln \left[\frac{\ln(1 - P_{fji})^{-1}}{\ln(1 - 0.5)^{-1}} \right] \right| \quad (20)$$

The process is iterative, covering an appropriate range of N_v values. The value of N_v associated with the minimum value of

$$MD_{\min} = \frac{1}{pq} \sum_{j=1}^q \sum_{i=1}^p \left| \ln t_{Tji} - \ln t_{T0.5} \right|$$

is the solution. Once the value of N_v has been determined, the Weibull modulus can be obtained for known P_{fji} since $\tilde{m}_v = m_v/(N_v - 2)$; hence

$$m_v = \frac{N_v - 2}{MD_{\min}} = \frac{1}{pq} \sum_{j=1}^q \sum_{i=1}^p \left| \ln \left[\frac{\ln(1 - P_{fji})^{-1}}{\ln(1 - 0.5)^{-1}} \right] \right| \quad (21)$$

After computing $g(\Psi_0)$ and V_{ef} , the value of $(B_{wv} \sigma_{ov}^{N_v-2})$ is then estimated from the median value $[\sigma_T(\Psi_0), t_{Tji}]_{0.5}$ via equation (17).

Dynamic fatigue.—For dynamic fatigue tests at a constant stress rate $\dot{\sigma}_j$, the time to failure of the i^{th} specimen is t_{fji} or, equivalently, the maximum stress at failure associated with $\dot{\sigma}_j$ is $\sigma_{fji}(\Psi_0)$. Replacing $\sigma_{ff}(\Psi_0)$ in equation (13) with $\sigma_{fji}(\Psi_0)$, t_{fji} with $\sigma_{fji}(\Psi_0)/\dot{\sigma}_j(\Psi_0)$, and $g(\Psi_0)$ with $1/(N_v + 1)$ yields

$$P_{fji} = 1 - \exp \left\{ - \left[\frac{\sigma_{fji}^{N_v+1}(\Psi_0) V_{ef}^{1/\tilde{m}_v}}{\dot{\sigma}_j(\Psi_0) B_{wv} (1 + N_v) \sigma_{ov}^{N_v-2}} \right]^{\tilde{m}_v} \right\} \quad (22)$$

Since $\dot{\sigma}_j$ is the independent variable, equation (22) becomes

$$\begin{aligned} & \frac{\ln \left[\ln \left(\frac{1}{1 - P_{fji}} \right) \right]}{m_v} - \ln \sigma_{fji}(\Psi_0) \\ &= \frac{1}{N_v} \left\{ \ln \sigma_{fji}(\Psi_0) + \frac{2 \ln \left[\ln \left(\frac{1}{1 - P_{fji}} \right) \right]}{m_v} - \ln \dot{\sigma}_j(\Psi_0) \right\} \\ & \quad + \frac{1}{N_v} \ln \left[\frac{V_{ef}^{(N_v-2)/m_v}}{(N_v+1) B_{wv} \sigma_{ov}^{N_v-2}} \right] \quad (23) \end{aligned}$$

At location Ψ_0 , since $\sigma_{fji} = \dot{\sigma}_j t_{fji}$, where t_{fji} is the time to failure of the i^{th} specimen under stress rate $\dot{\sigma}_j$, another form of equation (22) is

$$\begin{aligned} & \frac{2 \ln \left[\ln \left(\frac{1}{1 - P_{fji}} \right) \right]}{m_v} + \ln t_{fji} \\ &= N_v \left\{ \frac{\ln \left[\ln \left(1 - P_{fji} \right)^{-1} \right]}{m_v} - \ln \dot{\sigma}_j - \ln t_{fji} \right\} \\ & \quad - \ln \left[\frac{V_{ef}^{(N_v-2)/m_v}}{B_{wv} (1 + N_v) \sigma_{ov}^{N_v-2}} \right] \quad (24a) \end{aligned}$$

Similar to equation (14), equation (22) can be expressed as

$$\sigma_{fji}(\Psi_0) = \dot{\sigma}_j^{1/(N_v+1)}(\Psi_0) C_{ji}^{1/(N_v+1)}$$

Maintaining the same risk of rupture for the specimen uniaxial Weibull model, all $\sigma_{fji}(\Psi_0)$, $\dot{\sigma}_j(\Psi_0)$ are transformed into $\sigma_{Tji}(\Psi_0)$, $\dot{\sigma}_T(\Psi_0)$ via

$$\dot{\sigma}_T(\Psi_0) = \min \left[\dot{\sigma}_j(\Psi_0) \right] \quad (24b)$$

$$\sigma_{Tji}(\Psi_0) = \left(\frac{\dot{\sigma}_T(\Psi_0)}{\dot{\sigma}_j(\Psi_0)} \right)^{1/(N_v+1)} \sigma_{fji}(\Psi_0)$$

Thus

$$P_{fji} = 1 - \exp \left\{ - \left[\frac{\sigma_{Tji}^{N_v+1}}{\left[\frac{\dot{\sigma}_T B_{wv} \sigma_{ov}^{N_v-2}}{g(\Psi_0) V_{ef}^{1/\tilde{m}_v}} \right]^{\tilde{m}_v}} \right] \right\} \quad (25)$$

This form is used in conjunction with the MLE method with $\sigma_{Tji}^{N_v+1}$ as the variate.

For the median deviation method, transforming the data via equation (24b) results in the following:

$$\begin{aligned} MD_{\min} &= \frac{1}{pq} \sum_{j=1}^q \sum_{i=1}^p \left| \ln \sigma_{Tji} - \ln \sigma_{T0.5} \right| \\ &= \frac{1}{pq m_v} \left(\frac{N_v - 2}{N_v + 1} \right) \sum_{j=1}^q \sum_{i=1}^p \left| \ln \left[\frac{\ln \left(\frac{1}{1 - P_{fji}} \right)}{\ln 2} \right] \right| \quad (26) \end{aligned}$$

Parameter estimation methods I to VI are now applicable to the dynamic fatigue case.

Paris Law

Cyclic effects on slow crack growth are dependent on the duration and the number of cycles. Modeling for cyclic effects is based on phenomenological criteria (Paris law, Walker law) traditionally used for metal fatigue. As shown in a previous section, the Power law expresses the crack growth increment

per unit time. This section will describe the Paris law formulation, which expresses the crack growth increment per cycle.

Analysis.—The Paris law formulation describes the cyclic loading by incorporating in the analysis the difference between the maximum and minimum stress intensities. The rate equation is given as

$$\frac{da(\Psi, n)}{dn} = A_o \Delta K_{Ieq}^N(\Psi, n) \quad (27)$$

where A_o is a material fatigue parameter,

$$a(\Psi, n) = \left(\frac{K_{Ic}}{Y} \right)^2 \sigma_{Ieq, n}^{-2}(\Psi, n) \quad (28)$$

and

$$\begin{aligned} \Delta K_{Ieq}(\Psi, n) &= \left[\sigma_{Ieq, \max}(\Psi, n) - \sigma_{Ieq, \min}(\Psi, n) \right] Y \sqrt{a(\Psi, n)} \\ &= \sigma_{Ieq, \max}(\Psi, n) [1 - R(\Psi, n)] Y \sqrt{a(\Psi, n)} \end{aligned} \quad (29)$$

where R is the ratio of the minimum to maximum equivalent stress in a loading cycle,

$$R(\Psi, n) = \frac{\sigma_{Ieq, \min}}{\sigma_{Ieq, \max}}$$

and n is the number of cycles. From equations (27) to (29), the transformed stress becomes

$$\begin{aligned} \sigma_{Ieq, 0}(\Psi, n_f) &= \left\{ \frac{\int_0^{n_f} [1 - R(\Psi, n)]^{N_v} \sigma_{Ieq, \max}^{N_v}(\Psi, n) dn}{B} \right. \\ &\quad \left. + \sigma_{Ieq, \max}^{N_v - 2}(\Psi, n_f) \right\}^{1/(N_v - 2)} \end{aligned} \quad (30)$$

where

$$B = \frac{2}{A_o K_{Ic}^{N_v - 2} (N_v - 2) Y^2} \quad (31)$$

For a periodic cyclic stress, $R(\Psi, n)$ and $\sigma_{Ieq, \max}(\Psi, n)$ are independent of n ; hence,

$$\sigma_{Ieq, 0}(\Psi) = \left\{ \frac{\sigma_{Ieq, \max}^{N_v}(\Psi) [1 - R(\Psi)]^{N_v} n_f}{B} + \sigma_{Ieq, \max}^{N_v - 2}(\Psi, n_f) \right\}^{1/(N_v - 2)} \quad (32)$$

For $\left\{ \frac{\sigma_{Ieq, \max}^2(\Psi) [1 - R(\Psi)]^{N_v} n_f}{B} \right\} \gg 1$, equation (32) is approximated as

$$\sigma_{Ieq, 0}(\Psi) = \left\{ \frac{\sigma_{Ieq, \max}^{N_v}(\Psi) [1 - R(\Psi)]^{N_v} n_f}{B} \right\}^{1/(N_v - 2)} \quad (33)$$

Equation (33) represents the transformation of the stress distribution at $n = n_f$ to its inert stress distribution at $n = 0$.

The fatigue parameters N_v and B are obtained from cyclic rupture data tests on uniaxially loaded specimens. For a given value of j , associated with stress level $\sigma_{ff}(\Psi_0) = [\sigma_{Ieq, \max}(\Psi_0)]_j$, where Ψ_0 is the location of the maximum cyclic stress, the number of cycles to failure for the i^{th} specimen is n_{fji} . The data $\{\sigma_{ff}(\Psi_0) [1 - R_j(\Psi_0)], n_{fji}\}$ are ranked for each value of j , where j varies from 1 to q and i varies from 1 to p . For the i^{th} specimen of rank r subjected to stress level j , the failure probability is

$$P_{fji} = \frac{r - 0.3}{p + 0.4}$$

Maintaining the same risk of rupture for the specimen uniaxial Weibull model and the uniaxial Weibull model results in

$$P_{fji} = 1 - \exp \left[- \left(\frac{n_{fji} \left\{ [1 - R_j(\Psi_0)] \sigma_{ff}(\Psi_0) \right\}^{N_v}}{\left(\frac{B_{wv} \sigma_{ov}^{N_v - 2}}{V_{ef}^{1/\tilde{m}_v}} \right)} \right)^{\tilde{m}_v} \right] \quad (34)$$

and

$$n_{fji} = C_{ji} \left\{ \sigma_{ff}(\Psi_0) [1 - R_j(\Psi_0)] \right\}^{-N_v} \quad (35)$$

where

$$C_{ji} = \left\{ \frac{B_{wv} \sigma_{ov}^{N_v - 2}}{\left[\frac{V_{ef}}{\ln(1 - P_{fji})^{-1}} \right]^{1/\tilde{m}_v}} \right\} \quad (36)$$

and

$$V_{ef} = \int_v \left\{ \frac{\sigma_{ff}(\Psi) [1 - R_j(\Psi)]}{\sigma_{ff}(\Psi_0) [1 - R_j(\Psi_0)]} \right\}^{(N_v m_v)/(N_v - 2)} dV \quad (37)$$

From equation (35)

$$\ln(n_{fji}) = \ln C_{ji} - N_v \ln \left\{ \sigma_{ff}(\Psi_0) [1 - R_j(\Psi_0)] \right\} \quad (38)$$

and

$$\begin{aligned} \ln(n_{fji}) + \frac{2 \ln \left[\ln(1 - P_{fji})^{-1} \right]}{m_v} \\ = N_v \left(\frac{\ln \left[\ln(1 - P_{fji})^{-1} \right]}{m_v} - \ln \left\{ \sigma_{ff}(\Psi_0) [1 - R_j(\Psi_0)] \right\} \right) \\ - \ln \left(\frac{V_{ef}^{1/\tilde{m}_v}}{B_{wv} \sigma_{ov}^{N_v - 2}} \right) \quad (39) \end{aligned}$$

with $\sigma_{ff}(\Psi_0) [1 - R_j(\Psi_0)]$ the independent variable and n_{fji} the dependent variable. Maintaining the same risk of rupture for all data, $\{\sigma_{ff}(\Psi_0) [1 - R_j(\Psi_0)], n_{fji}\}$ are transformed into $\{\sigma_T(\Psi_0) [1 - R_T(\Psi_0)], n_{Tji}\}$,

where

$$\sigma_T(\Psi_0) [1 - R_T(\Psi_0)] = \min \left\{ \sigma_{ff}(\Psi_0) [1 - R_j(\Psi_0)] \right\}$$

$$n_{Tji} = \left\{ \frac{\sigma_{ff}(\Psi_0) [1 - R_j(\Psi_0)]}{\sigma_T(\Psi_0) [1 - R_T(\Psi_0)]} \right\}^{N_v} n_{fji} \quad (40)$$

and substituting into equation (34),

$$P_{fji} = 1 - \exp \left\{ - \left[\frac{n_{Tji}}{\left(\frac{B_{wv} \sigma_{ov}^{N_v - 2}}{\left\{ \sigma_T(\Psi_0) [1 - R_T(\Psi_0)] \right\}^{N_v} V_{ef}^{1/\tilde{m}_v}} \right)} \right]^{\tilde{m}_v} \right\} \quad (41)$$

Parameter estimation.—The following are techniques which may be used to determine the parameters for cyclic fatigue using the Paris law formulation just described.

Method I—Least-squares best fit using median values. The inert parameters m_v and σ_{ov} are known. For the median values, equation (38) becomes

$$\ln(n_{fji})_{0.5} = \ln(C_{ji})_{0.5} - N_v \ln \left\{ \sigma_{ff}(\Psi_0) [1 - R_j(\Psi_0)] \right\}_{0.5}$$

where the subscript 0.5 denotes the median value. Since $P_{fji} = 0.5$, the intercept $\ln(C_{ji})_{0.5}$ is a constant. Substituting the set of median values into the above equation determines N_v and $(C_{ji})_{0.5}$; V_{ef} is computed and B_{wv} is found from the value of the intercept.

Method II—Maximum likelihood estimation using median values. The inert parameters are known. An initial value of N_v is assumed based on a least-squares best-fit regression analysis; $\{\sigma_{ff}(\Psi_0) [1 - R_j(\Psi_0)], n_{fji}\}_{0.5}$ are transformed via equation (40) to the data set $\{\sigma_T(\Psi_0) [1 - R_T(\Psi_0)], n_{Tji}\}_{0.5}$. The maximum likelihood estimation method is applied to equation (41) with $(n_{Tji})_{0.5}$ as the variate; then the value of \tilde{m}_v is obtained. From this value, N_{assumed} is compared with N_{computed} . The process is iterative. When both values are within some specified tolerance, the solution for N_v has been found. After convergence, V_{ef} and B_{wv} are evaluated.

Method III—Least-squares best fit using all fatigue rupture data. The inert parameters are known. The data for each value of $\sigma_{ff}(\Psi_0) [1 - R_j(\Psi_0)]$ are ranked in accordance with the magnitude of n_{fji} to obtain the data set $\{\sigma_{ff}(\Psi_0) [1 - R_j(\Psi_0)], n_{fji} P_{fji}\}$. These values are substituted in equation (39) to evaluate N_v and the intercept; V_{ef} is determined and from the value of the intercept, B_{wv} is obtained.

Method IV—Maximum likelihood estimation using all fatigue rupture data: The inert parameters are known. A value $N_v = N_{\text{assumed}}$ is assumed based on the least-squares best-fit results. The data are transformed through equation (40) to data set $\{\sigma_T(\Psi_0) [1 - R_T(\Psi_0)], n_{Tji}\}$. The maximum likelihood estimation method is applied to equation (41) with n_{Tji} as the variate to solve for \tilde{m}_v . The value of N_v is computed and then compared with the assumed value. These two values are averaged and the process is repeated until the assumed value is within some specified tolerance of the computed value; V_{ef} and B_{wv} are evaluated.

Method V—Least-squares best fit to evaluate unsubscripted B: The value of B , equation (31), that is not model dependent can be obtained using all the rupture data (inert plus fatigue). Introducing the subscripts i and j into equation (33) with reference to specimen number and stress level, respectively, yields

$$\sigma_{1ji,0}^{N_v-2}(\Psi_0) = \left\{ \frac{\sigma_{fj}^{N_v}(\Psi_0) [1 - R_j^{N_v}(\Psi_0)] n_{fji}}{B} \right\} \quad (42)$$

and

$$\ell n n_{fji} + 2 \ell n \sigma_{1ji,0}(\Psi_0) = N_v \left(\ell n \sigma_{1ji,0}(\Psi_0) - \ell n \left\{ \sigma_{fi}(\Psi_0) [1 - R_j(\Psi_0)] \right\} \right) + \ell n B \quad (43)$$

where $\sigma_{1ji,0}(\Psi_0)$ is the inert maximum principal stress associated with n_{fji} by the equivalence of rank. Thus, the inert stress $\sigma_{1ji,0}$ is matched with $\{\sigma_{fj}(\Psi_0) [1 - R_j(\Psi_0)], n_{fji}\}$. The above equation is used to solve for N_v , and from the intercept, evaluate B .

Method VI—Median deviation: The median deviation measures the spread of the data about the median value. The median deviation method is used when the inert parameters are unknown and only subcritical crack growth rupture data are available. From the minimization of the median deviation, the material parameters m_v , N_v , and the product $B_{wv} \sigma_{ov}^{N_v-2}$ are evaluated. For an assumed value of N_v , the data $\{\sigma_{fj}^{N_v}(\Psi_0) [1 - R_j(\Psi_0)], n_{fji}\}$ are transformed via equation (40) into $\{\sigma_T(\Psi_0) [1 - R_T(\Psi_0)], n_{Tji}\}$. From the transformed data, the median deviation for the total number of data points qp is

$$MD = \frac{1}{pq} \sum_{j=1}^q \sum_{i=1}^p \left| \ell n n_{Tji} - \ell n n_{T0.5} \right|$$

$$= \frac{1}{\tilde{m}_v pq} \sum_{j=1}^q \sum_{i=1}^p \left| \ell n \left[\frac{\ell n(1 - P_{fji})^{-1}}{\ell n(1 - 0.5)^{-1}} \right] \right| \quad (44)$$

The process is iterative, covering an appropriate range of N_v values. The value of N_v associated with the minimum value of the median deviation MD_{\min} is the solution. With N_v and P_{fji} known,

$$m_v = \frac{N_v - 2}{MD_{\min}} \frac{1}{pq} \sum_{j=1}^q \sum_{i=1}^p \left| \ell n \left[\frac{\ell n(1 - P_{fji})^{-1}}{\ell n(1 - 0.5)^{-1}} \right] \right| \quad (45)$$

The value of $B_{wv} \sigma_{ov}^{N_v-2}$ is then estimated from the median value $\{\sigma_T(\Psi_0) [1 - R_T(\Psi_0)], n_{Tji}\}_{0.5}$ via equation (41).

Walker Law

Analysis.—As illustrated in the previous section, the Paris law formulation describes the cyclic loading by incorporating in the analysis the difference between the maximum and minimum stress intensities. However, this approach does not take into account the effect of the stress ratio R (i.e., the ratio of the minimum to maximum cyclic stress). For metals, it was observed that the higher the positive value of R , the greater the amount of crack growth. To incorporate the effect of stress ratio on crack growth, the Walker formulation is used. The Walker law rate equation is given as

$$\frac{da(\Psi, n)}{dn} = A_o K_{Ieq}^{Q_v - N_v}(\Psi, n) \Delta K_{Ieq}^{N_v} = \frac{A_o \Delta K_{Ieq}^{Q_v}(\Psi, n)}{[1 - R(\Psi, n)]^{Q_v - N_v}} \quad (46)$$

where $K_{Ieq} = K_{Ieqc_{\max}}$ and Q_v is the Walker material fatigue parameter. When Q_v equals N_v , the Walker law reduces to the Paris law:

$$\Delta K_{Ieq} = Y \sigma_{Ieqc_{\max}}(\Psi, n) [1 - R(\Psi, n)] \sqrt{a(\Psi, n)} \quad (47)$$

where

$$R(\Psi, n) = \frac{\sigma_{Ieqc_{\min}}(\Psi, n)}{\sigma_{Ieqc_{\max}}(\Psi, n)}$$

and

$$a(\Psi, n) = \left(\frac{K_{Ic}}{Y} \right)^2 \sigma_{Ieqc,n}^{-2}(\Psi, n) \quad (48)$$

where n is the number of cycles. From equations (46) to (48), we obtain the transformed equivalent stress distribution at $n = n_f$ to its equivalent inert stress distribution at $n = 0$:

$$\sigma_{Ieqc,0}(\Psi) = \sigma_{Ieqc,n}(\Psi, n=0)$$

$$= \left\{ \frac{\int_0^{n_f} \sigma_{Ieqc_{max}}^{Q_v}(\Psi, n) [1 - R(\Psi, n)]^{N_v} dn}{B} + \sigma_{Ieqc_{max}}^{Q_v-2}(\Psi, n_f) \right\}^{1/(Q_v-2)} \quad (49)$$

where

$$B = \frac{2}{A_o Y^2 (Q_v - 2) K_{Ic}^{Q_v-2}}$$

For $\sigma_{Ieqc_{max}}(\Psi, n)$ and $R(\Psi, n)$, independent of n ,

$$\sigma_{Ieqc,0}(\Psi) = \left\{ \frac{\sigma_{Ieqc_{max}}^{Q_v}(\Psi) [1 - R(\Psi)]^{N_v} n_f}{B} + \sigma_{Ieqc_{max}}^{Q_v-2}(\Psi) \right\}^{1/(Q_v-2)} \quad (50)$$

For $\left\{ \sigma_{Ieqc_{max}}^2(\Psi) [1 - R(\Psi)]^{N_v} n_f / B \right\} \gg 1$,

$$\sigma_{Ieqc,0} = \left\{ \frac{\sigma_{Ieqc_{max}}^{Q_v}(\Psi) [1 - R(\Psi)]^{N_v} n_f}{B} \right\}^{1/(Q_v-2)} \quad (51)$$

The fatigue parameters N_v , Q_v , and B are obtained from cyclic rupture data on uniaxially loaded specimens. For a given value of j , associated with $\sigma_{ff}(\Psi_0) = [\sigma_{Ieqc_{max}}(\Psi_0)]_j$ the maximum principal stress in the specimen, the number of cycles to failure of the i^{th} specimen is n_{fji} . The data $\{ \sigma_{ff}(\Psi_0) [1 - R_j(\Psi_0)], n_{fji} \}$ are ranked for each value of j , where j varies from 1 to q and i varies from 1 to p . For the i^{th} specimen of rank r , $P_{fji} = (r - 0.3) / (p + 0.4)$. With this subscript notation, equation (51) becomes

$$\sigma_{Iji,0}(\Psi_0) = \left\{ \frac{\sigma_{ff}^{Q_v}(\Psi_0) [1 - R_j(\Psi_0)]^{N_v} n_{fji}}{B} \right\}^{1/(Q_v-2)} \quad (52)$$

Equation (52) represents the transformation of the maximum principal stress σ_{ff} at n_{fji} to the inert stress $\sigma_{Iji,0}$ at $n = 0$. Maintaining the same risk of rupture for the specimen uniaxial Weibull model and the uniaxial Weibull model results in

$$P_{fji} = 1 - \exp \left[- \left(\frac{n_{fji}}{\left\{ \frac{B_{wv} \sigma_{ov}^{Q_v-2}}{\sigma_{ff}^{Q_v}(\Psi_0) [1 - R_j(\Psi_0)]^{N_v} V_{ef}^{(Q_v-2)/m_v}} \right\}} \right)^{m_v / (Q_v-2)} \right] \quad (53a)$$

and

$$n_{fji} = C_{ji} \sigma_{ff}^{-Q_v}(\Psi_0) [1 - R_j(\Psi_0)]^{-N_v} \quad (53b)$$

where

$$C_{ji} = \frac{\sigma_{ov}^{Q_v-2} B_{wv}}{\left[\frac{V_{ef}}{\ln(1 - P_{fji})^{-1}} \right]^{(Q_v-2)/m_v}}$$

and

$$V_{ef} = \int_v \left\{ \frac{\sigma_{ff}^{Q_v}(\Psi) [1 - R_j(\Psi)]^{N_v}}{\sigma_{ff}^{Q_v}(\Psi_0) [1 - R_j(\Psi_0)]^{N_v}} \right\}^{m_v / (Q_v-2)} dv$$

From equations (53),

$$\ln n_{fji} = \ln C_{ji} - Q_v \ln \sigma_{ff}(\Psi_0) - N_v \ln [1 - R_j(\Psi_0)] \quad (54)$$

and

$$\ln n_{fji} + \frac{2 \ln \left[\ln(1 - P_{fji})^{-1} \right]}{m_v} = Q_v \left\{ \frac{\ln \left[\ln(1 - P_{fji})^{-1} \right]}{m_v} - \ln \sigma_{ff}(\Psi_0) \right\} - N_v \ln [1 - R_j(\Psi_0)] + \ln \left(\frac{\sigma_{ov}^{Q_v-2} B_{wv}}{V_{ef}^{(Q_v-2)/m_v}} \right) \quad (55)$$

Maintaining the same risk of rupture for the specimen uniaxial Weibull model, all fatigue rupture data $\{\sigma_{ff}(\Psi_0) [1 - R_j(\Psi_0)], n_{fji}\}$ are transformed to an equivalent data set $\{\sigma_T(\Psi_0) [1 - R_T(\Psi_0)], n_{Tji}\}$ for given values of Q_v and N_v :

$$n_{Tji} = \left\{ \frac{\sigma_{ff}^{Q_v}(\Psi_0) [1 - R_j(\Psi_0)]^{N_v}}{\sigma_T^{Q_v}(\Psi_0) [1 - R_T(\Psi_0)]^{N_v}} \right\} n_{fji} \quad (56)$$

where $\sigma_T(\Psi_0)$ and $R_T(\Psi_0)$ are the lowest values of the set of data $\{\sigma_{ff}(\Psi_0) [1 - R_j(\Psi_0)]\}$. Substituting equation (56) into equation (53) yields

$$P_{fji} = 1 - \exp \left[- \left(\frac{n_{Tji}}{\left\{ \frac{\sigma_{ov}^{Q_v-2} B_{wv}}{\left[\sigma_T^{Q_v}(\Psi_0) [1 - R_T(\Psi_0)]^{N_v} V_{ef}^{(Q_v-2)/m_v} \right]} \right\}} \right)^{m_v/(Q_v-2)} \right] \quad (57)$$

Parameter estimation.—The following are techniques which may be used to determine the parameters for cyclic fatigue using the Walker law formulation just described.

Method I—Least-squares best-fit regression plane using median values: The inert parameters σ_{ov} and m_v are known. The data median values $(\sigma_{ff}(\Psi_0) [1 - R_j(\Psi_0)], n_{fji})_{0.5}$ are substituted into equation (54); $P_{fji} = 0.5$ and C_{ji} is now constant; C_{ji} , Q_v , N_v are computed via the least-squares best-fit regression plane analysis; V_{ef} and B_{wv} are then evaluated.

Method II—Least-squares best-fit regression plane using all data: The inert parameters σ_{ov} and m_v are known. For each value of j from the data, ranked in accordance with the value of n_{fji} , the values of P_{fji} associated with $\{\sigma_{ff}(\Psi_0) [1 - R_j(\Psi_0)], n_{fji}\}$ are obtained. From a least-squares best-fit analysis of the data applied to equation (55), Q_v and N_v are computed; V_{ef} and B_{wv} are then evaluated.

Method III—Least-squares best-fit regression plane to evaluate unsubscripted B: The value of B in equation (49) is not model dependent and can be obtained using all the rupture data (inert and subcritical crack growth). The transformed maximum principal uniaxial stress $\sigma_{1ji,0}(\Psi_0)$ in equation (52) is taken as the inert strength distribution. The inert strength is associated with $\{\sigma_{ff}(\Psi_0) [1 - R_j(\Psi_0)], n_{fji}\}$ by equivalence of rank. For each j varying from 1 to q , the subscript i varies from 1 to p . There are p -specimens tested for each value of j . From equation (52),

$$\begin{aligned} \ell n n_{fji} + 2 \ell n \sigma_{1ji,0}(\Psi_0) = Q_v \left[\ell n \sigma_{1ji,0}(\Psi_0) - \ell n \sigma_{ff}(\Psi_0) \right] \\ - N_v \ell n [1 - R_j(\Psi_0)] + \ell n B \quad (58) \end{aligned}$$

The data are substituted into equation (58) to solve for Q_v , N_v , and B .

Method IV—Maximum likelihood estimation using all data: This iterative process involves determining values Q_v , N_v , and B_{wv} assumed unique to the data. The inert parameters are known. Based on LSBF results, the values $N_v = N_{\text{assumed}}$ and $Q_v = Q_{\text{assumed}}$ are assumed. The data are transformed via equation (56). The MLE method is applied to equation (57), with n_{Tji} as the variate to solve for $m_v/(Q_v-2)$ and then to compute Q_v . This value is then compared with the assumed value. If Q_{computed} is within a specified tolerance of Q_{assumed} , the solution is obtained. If not, the next value of Q_v is assumed to be the average of these two values. If no solution exists, the process is restarted with a new value for N_{assumed} .

Experimental Applications

The examples in this section employ some of the equations presented in the preceding theoretical sections. It is understood in this section that failure occurs at location Ψ_0 , and therefore said notation will be omitted in the subsequently developed equations. Inert room-temperature and dynamic fatigue fracture data are analyzed for (a) soda lime glass, ring-on-ring square plate test specimens and (b) sintered alpha silicon carbide (SASC) material obtained from O-ring and C-ring specimens at 1200 and 1300 °C.

For the soda lime glass material, inert parameters are obtained using the least-squares best-fit (LSBF) and maximum likelihood estimation (MLE) methods. Dynamic fatigue data are then utilized in conjunction with these known inert parameters (obtained via the LSBF and MLE methods) to generate fatigue parameters for the soda lime glass. This approach was used to determine fatigue parameters for the LSBF method. The MLE method did not converge to a solution. The results of these methods are presented. Finally, the soda lime glass dynamic fatigue data are used in conjunction with the median deviation (MD) method to obtain the cumulative distribution curve defined by the Weibull parameter m_s , the fatigue parameters N_s , and the product $B_{ws} \sigma_{os}^{N_s-2}$.

For the sintered alpha silicon carbide material, inert parameters are obtained using the least-squares best-fit (LSBF) and maximum likelihood estimation (MLE) methods. Dynamic fatigue data are then utilized in conjunction with these known inert parameters (obtained via the LSBF and MLE methods) to generate fatigue parameters for the SASC material.

Simulations have shown (ref. 11) that the standard deviation for the MLE method is smaller than that for the LSBF method. However, all experimental data reflect some degree of error (ref. 12) and flaw variability. Both methods (MLE and LSBF) are used in the determination of the relevant parameters.

Soda Lime Glass

Inert data (table II) and dynamic fatigue data (table III) were obtained from soda lime glass ring-on-ring specimens (fig. 1). For this material, inherent surface flaws were the source of failure (Nemeth, N.N. et al.: CARES/LIFE Ceramic Analysis and Reliability Evaluation of Structures Life Prediction Program. NASA Lewis Research Center, unpublished data, 1993). The radial stress σ_r and tangential stress σ_{\tan} on the tensile loaded surface are equal for radius $r \leq R_i$, the radius of the load ring

$$\sigma_{\tan} = \sigma_r = \frac{3P}{4\pi h^2} \left[2(1+\nu) \ln\left(\frac{R_o}{R_i}\right) + \frac{(1+\nu)(R_o^2 - R_i^2)}{R_s^2} \right] \quad (59)$$

where P is the applied load, h is the specimen thickness, ν is Poisson's ratio, and R_s is the diagonal half-length of the square plate specimen (fig. 1). The maximum principal stress for $r \geq R_i$ is the tangential stress

$$\sigma_{\tan} = \frac{3P}{4\pi h^2} \left[2(1+\nu) \ln\left(\frac{R_o}{r}\right) - (1-\nu) \frac{(R_o^2 + r^2)}{r^2} \left(\frac{R_i}{R_s}\right)^2 + 2(1-\nu) \left(\frac{R_o}{R_s}\right)^2 \right] \quad (60)$$

Inert data analysis.—For the soda lime glass material, inert parameters are obtained using the least-squares best-fit and maximum likelihood estimation methods.

For the least-squares best-fit method applied to the inert data,

$$\ln \left[\ln \left(\frac{1}{1 - P_{ff}} \right) \right] = m_s \ln \sigma_{ff} - m_s \ln \sigma_{\theta_s} \quad (61)$$

where P_{ff} is the probability of failure of the j^{th} specimen, obtained from the ranking of σ_{ff} ; m_s is the Weibull modulus; σ_{ff} is the maximum tangential stress at failure of the j^{th} specimen; and σ_{θ_s} is the characteristics strength. Figure 2 shows a plot of the ring-on-ring inert data and the solution obtained using the LSBF method.

For the maximum likelihood estimation method applied to the inert data,

$$P_{ff} = 1 - \exp \left[- \left(\frac{\sigma_{ff}}{\sigma_{\theta_s}} \right)^{m_s} \right] \quad (62)$$

TABLE II.—INERT DATA FROM SODA LIME GLASS RING-ON-RING SPECIMENS

Thickness, h , mm	Fracture load, P , kN	Thickness, h , mm	Fracture load, P , kN
1.0990	1.5420	0.4285	1.4150
1.4830	1.4520	.6478	1.5510
1.5540	1.5420	.7980	1.4920
1.3650	1.5220	.5124	1.4340
1.2910	1.5050	.7424	1.5250
.8305	1.5340	1.5070	1.5180
.9756	1.4920	.8223	1.4430
1.7910	1.5190	1.4640	1.5260
.5491	1.4480	1.0920	1.4780
1.9000	1.5320	1.2260	1.5170
.6928	1.5310	1.3110	1.4750
.6418	1.5660	1.8130	1.5590
.4529	1.4950	1.4800	1.5260
.6357	1.4940	1.5880	1.5450
.6153	1.4370	1.5230	1.4950

TABLE III.—DYNAMIC FATIGUE DATA FROM SODA LIME GLASS RING-ON-RING SPECIMENS

Fracture stress, σ , MPa (at various stress rates, $\dot{\sigma}$, MPa/sec)			
σ_{fi} at $\dot{\sigma}_1 = 0.02$	σ_{fi} at $\dot{\sigma}_2 = 0.20$	σ_{fi} at $\dot{\sigma}_3 = 2.00$	σ_{fi} at $\dot{\sigma}_4 = 20.00$
188.677	138.963	239.176	267.279
43.414	186.046	324.237	250.898
238.163	53.900	112.060	302.116
163.981	226.200	69.959	200.791
214.390	228.609	224.201	85.021
180.811	110.241	360.756	533.321
206.690	355.705	174.677	307.547
135.819	59.525	312.900	282.393
198.489	231.543	182.485	377.911
273.027	63.768	271.662	311.192
143.526	312.097	311.681	172.435
113.158	184.891	226.959	202.541
212.336	255.119	99.672	253.662
137.096	245.585	164.974	339.116
67.769	112.365	104.515	211.909
246.808	164.962	286.925	259.588
247.317	162.755	264.994	237.630
189.628	150.471	109.795	302.684
164.883	77.447	133.134	360.206
114.253	151.813	321.845	310.427
216.749	215.165	136.249	293.215
216.407	129.921	140.760	138.294
97.967	135.024	213.386	320.906
98.705	128.776	234.744	269.308
132.668	136.033	373.915	470.079
108.464	268.623	313.608	252.308
120.170	241.587	269.948	257.600
169.924	236.632	288.936	335.608
172.539	177.639	227.179	223.475
246.477	188.238	326.009	428.672
-----	191.009	-----	-----

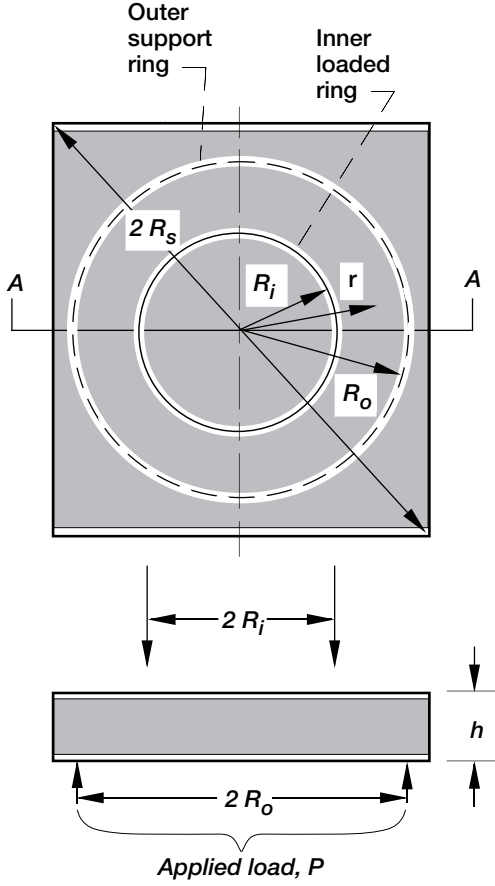


Figure 1.—Ring-on-ring loaded square plate specimen. Poisson's ratio, ν , 0.22; outer ring radius, R_o , 16.090 mm; inner ring radius, R_i , 5.015 mm; diagonal half-length, R_s , 35.921 mm.

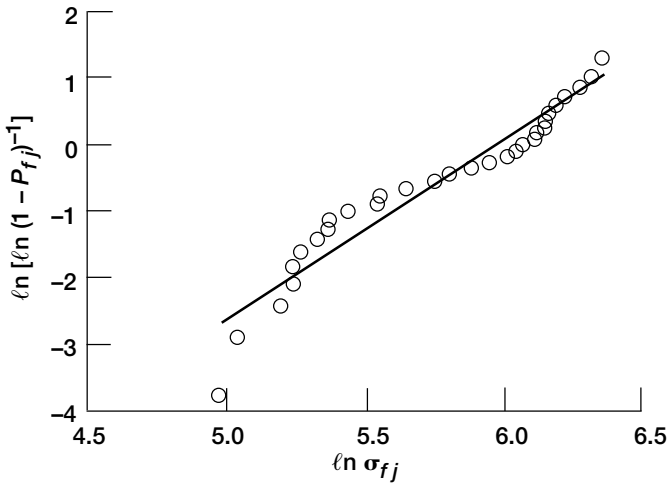


Figure 2.—Ring-on-ring inert data and least-squares best-fit line. Weibull modulus, m_s , 2.675; scale factor, σ_{os} , 15.76 MPa-m^{2/m_s}; effective area, A_e , 191.0 mm².

For j varying from 1 to q (q = total number of test specimens),

$$m_s = \frac{q \sum_{j=1}^q \sigma_{fj}^{m_s}}{q \sum_{j=1}^q \sigma_{fj}^{m_s} \ln \sigma_{fj} - \sum_{j=1}^q \ln \sigma_{fj} \sum_{j=1}^q \sigma_{fj}^{m_s}} \quad (63)$$

and

$$\sigma_{\theta s} = \left(\frac{\sum_{j=1}^q \sigma_{fj}^{m_s}}{q} \right)^{1/m_s} \quad (64)$$

The scale factor is $\sigma_{os} = \sigma_{\theta s} A_e^{1/m_s}$, where the effective area is

$$A_e = \int_A \left(\frac{\sigma_{fj}(r)}{\sigma_{fj}(r=0)} \right)^{m_s} dA \quad (65)$$

and $\sigma_{fj}(r) = \sigma_{\tan}(r)$ is the maximum principal tangential stress distribution. Figure 3 shows a plot of the ring-on-ring inert data and the solution obtained using the MLE method.

Dynamic fatigue data analysis.—In this section, fatigue parameters are determined using dynamic fatigue data in conjunction with known inert parameters m_s and σ_{os} (obtained via the LSBF and MLE methods). The effective area A_{ef} is assumed constant for all specimens.

For the least-squares best-fit method applied to the dynamic fatigue data, equation (22) is utilized for surface flaws by replacing subscript v with s . After some algebraic manipulation, where $\dot{\sigma}$ is the independent variable, the linear regression function is given by

$$\begin{aligned} & \frac{\ln \left[\ln \left(\frac{1}{1 - P_{fji}} \right) \right]}{m_s} - \ln \sigma_{fji} \\ &= \frac{1}{N_s} \left\{ \ln \sigma_{fji} + \frac{2 \ln \left[\ln \left(\frac{1}{1 - P_{fji}} \right) \right]}{m_s} - \ln \dot{\sigma}_j \right\} \\ &+ \frac{1}{N_s} \ln \left(\frac{A_{ef}^{(N_s-2)/m_s}}{(N_s+1) B_{ws} \sigma_{os}^{N_s-2}} \right) \quad (66) \end{aligned}$$

where the effective area is

$$A_{ef} = \int_A \left(\frac{\sigma_{fji}(r)}{\sigma_{fji}(r=0)} \right)^{(m_s N_s)/(N_s-2)} dA \quad (67)$$

Figure 4 is a plot of the ring-on-ring dynamic fatigue data; also shown is the solution obtained using the LSBF method applied to the median data values given in table IV. Figure 5 is a plot of the ring-on-ring dynamic fatigue data and shows the solution, obtained using the LSBF method, to all the dynamic fatigue data given in table III.

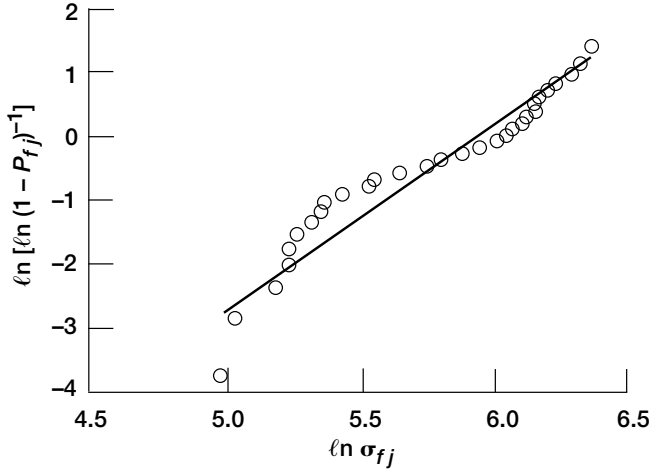


Figure 3.—Ring-on-ring inert data and maximum likelihood estimation line. Weibull modulus, m_s , 2.869; scale factor, σ_{os} , 19.20 MPa-m²/ m_s ; effective area, A_e , 182.6 mm².

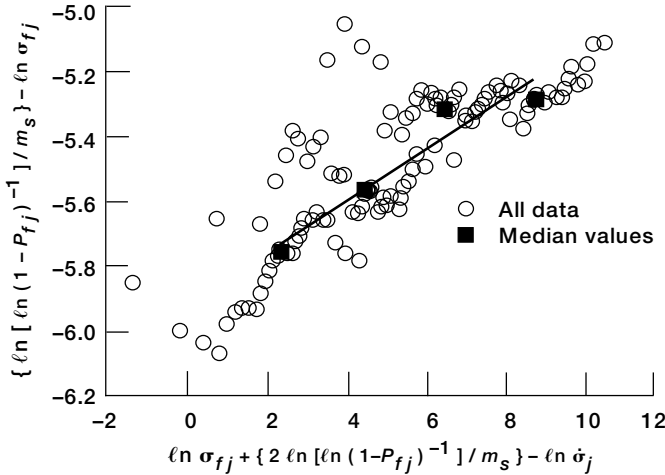


Figure 4.—Ring-on-ring dynamic fatigue data and least-squares best fit to median data values. Weibull modulus, m_s , 2.675; scale factor, σ_{os} , 15.76 MPa-m²/ m_s ; exponential fatigue parameter, N_s , 12.68; Weibull fatigue parameter, B_{ws} , 1.21 MPa²-hr; effective area, A_{ef} , 171.4 mm².

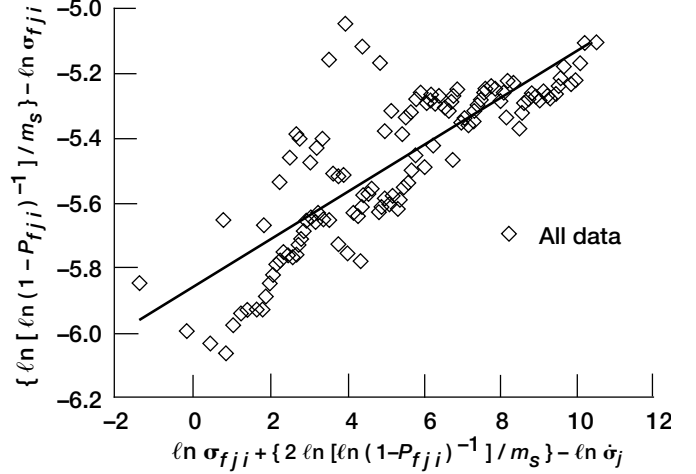


Figure 5.—Ring-on-ring least-squares best fit to all dynamic fatigue data. Weibull modulus, m_s , 2.675; scale factor, σ_{os} , 15.76 MPa-m²/ m_s ; exponential fatigue parameter, N_s , 13.84; Weibull fatigue parameter, B_{ws} , 0.468 MPa²-hr; effective area; A_{ef} , 173.0 mm².

TABLE IV.—DYNAMIC FATIGUE MEDIAN VALUES FROM SODA LIME GLASS RING-ON-RING SPECIMEN^a

Stress rate, $\dot{\sigma}_j$, MPa/sec	Tangential fracture stress, σ_{ff} , MPa
0.02	171.23
.20	177.64
2.00	230.96
20.00	275.85

^aShown in fig. 1.

If the effective area A_{ef} is not constant (i.e., A_{effi}), equation (66) can be written in another form:

$$\frac{\ln \left[\ln \left(\frac{1}{1 - P_{fji}} \right) \right]}{m_s} - \ln \sigma_{fji} + \ln \sigma_{os} = -\frac{1}{N_s} \left[\ln(N_s + 1) \right. \\ \left. + \ln B_{ws} \right] + \frac{1}{N_s} \left\{ \ln \sigma_{fji} + \frac{2 \ln \left[\ln \left(\frac{1}{1 - P_{fji}} \right) \right]}{m_s} - \ln \dot{\sigma}_j \right. \\ \left. + \frac{N_s - 2}{m_s} \ln A_{effi} + 2 \ln \sigma_{os} \right\} \quad (68)$$

The process for computing N_s is iterative. The value of A_{effi} is assumed to be constant for all specimens (A_{effi} is constant). This constant value is used to calculate a starting value for N_s (eq. (66)). Then, this starting value of N_s and the specimen A_{effi} values are used to begin the iterative process. Iteration continues until the assumed value of N_s is equal to (or within some specified tolerance of) the computed value of N_s .

Since $\sigma_{fji} = \dot{\sigma}_j t_{fji}$, where t_{fji} is the time to failure of the i^{th} specimen under stress rate $\dot{\sigma}_j$, another form of equation (66) for surface flaws is

$$\begin{aligned} & \frac{2 \ln \left[\ln \left(\frac{1}{1 - P_{fji}} \right) \right]}{m_s} + \ln t_{fji} \\ &= N_s \left\{ \frac{\ln \left[\ln \left(\frac{1}{1 - P_{fji}} \right) \right]}{m_s} - \ln t_{fji} - \ln \dot{\sigma}_j \right\} \\ & \quad - \ln \left(\frac{A_{ef}^{(N_s-2)/m_s}}{(N_s+1)B_{ws}\sigma_{os}^{N_s-2}} \right) \quad (69) \end{aligned}$$

For the maximum likelihood estimation method applied to the dynamic fatigue data, with m_s and σ_{os} known, analogous to equations (62) and (22) is

$$P_{fji} = 1 - \exp \left[- \left(\frac{S_{fji}}{Z} \right)^{m_s} \right] \quad (70)$$

where the variate S_{fji} is

$$S_{fji} = \left(\frac{\sigma_{fji}^{N_s+1}}{\dot{\sigma}_j} \right)^{1/(N_s-2)}$$

and parameter Z is

$$Z = \left[\frac{(N_s+1)B_{ws}\sigma_{os}^{N_s-2}}{A_{ef}^{(N_s-2)/m_s}} \right]^{1/(N_s-2)}$$

The value of P_{fji} is obtained from the ranking of the failure stress.

The solution is obtained by assuming an appropriate range of values for N_s based on the least-squares best-fit result. With the value of N_s fixed, a starting value for m_s is assumed equal to the inert value. Based on this value, a computed Weibull modulus m_{sc} is obtained. A new value of m_s is assumed equal to $(m_s + m_{sc})/2$, and the process is repeated until convergence. Convergence is assumed to occur when the absolute value of the difference $(m_s - m_{sc})$ is < 0.01 . The process is repeated, changing the assumed value of N_s until the computed value of m_{sc} is equal to the known inert value. For the soda lime glass dynamic fatigue data examined here, this convergence did not occur, as shown in figure 6. The inert value of the Weibull modulus obtained via the maximum likelihood method is 2.869. At the start, for a fixed value of $N_s = 4$ and an assumed $m_s = 2.675$, convergence occurred after six iterations to $m_{sc} = 0.856$. In most cases, convergence occurred after two iterations. For N_s varying from 4 to 44, the largest value of m_{sc} obtained was 2.570. The computed modulus did not converge to the inert value of the Weibull modulus, 2.869.

The value of B_{us} for the ring-on-ring square plate test specimen is obtained via the specimen uniaxial Weibull model and least-squares best-fit method. The stress transformation equation is

$$\sigma_{Ieq,0}(\Psi_0) = \left[\frac{\sigma_{fji}^{N_s+1}(\Psi_0)}{\dot{\sigma}_j B_{us} (N_s+1)} \right]^{1/(N_s-2)} \quad (71)$$

Thus, the probability of failure is expressed as

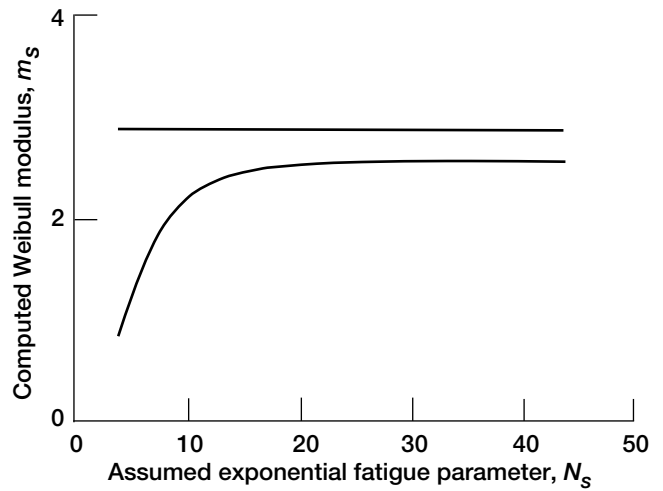


Figure 6.—Fatigue parameter determination for soda lime glass data via maximum likelihood estimation method. No convergence. Weibull modulus, m_s , 2.869; scale factor, σ_{os} , 19.20 MPa-m²/ m_s .

$$P_{fji} = 1 - \exp \left\{ - \left[\frac{\sigma_{Ieq,0}(\Psi_0)}{\sigma_{\theta_s}} \right]^{m_s} \right\}$$

$$= 1 - \exp \left\{ - \left[\frac{\sigma_{fji}^{N_s+1}(\Psi_0)}{\dot{\sigma}_j B_{us} (N_s + 1) \sigma_{\theta_s}^{N_s-2}} \right]^{m_s / (N_s - 2)} \right\} \quad (72)$$

and

$$\frac{\ell n \left[\ell n \left(\frac{1}{1 - P_{fji}} \right) \right]}{m_s} - \ell n \sigma_{fji}$$

$$= \frac{1}{N_s} \left\{ \ell n \sigma_{fji} + \frac{2}{m_s} \ell n \left[\ell n \left(\frac{1}{1 - P_{fji}} \right) \right] - \ell n \dot{\sigma}_j \right\}$$

$$- \frac{\ell n \left[(N_s + 1) B_{us} \sigma_{\theta_s}^{N_s-2} \right]}{N_s} \quad (73)$$

becomes the basis for a least-squares best-fit evaluation. Equating the risk of rupture of the specimen uniaxial Weibull model to that of the uniaxial Weibull model yields the relationship

$$B_{us} = B_{ws} \left(\frac{A_e}{A_{ef}} \right)^{(N_s - 2) / m_s}$$

For large values of N_s , A_{ef} tends toward A_e and B_{us} tends toward B_{ws} .

For the median deviation method applied to the soda lime glass dynamic fatigue data, it is assumed that no inert data are available. From equation (26) (for surface flaws replace subscript v with s), the value of $N_s = 13.1$ produces the minimum value MD_{min} . Figure 7 shows the variation of the MD value as a function of the assumed value of N_s . For assumed values of N_s that are less than 10.0 and greater than 13.1, the MD value continuously increases. A plot of the distribution solution versus the experimental fatigue data is given in figure 8.

Sintered Alpha Silicon Carbide (SASC)

Inert data (table V) and dynamic fatigue data (table VI) were obtained from sintered alpha silicon carbide O-ring and C-ring specimens tested at temperatures of 1200 and 1300°C. Schematic

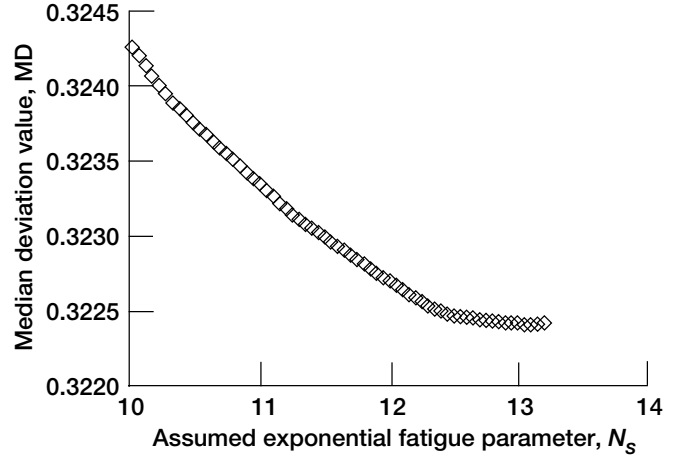


Figure 7.—Median deviation sum (MD) as function of assumed exponential fatigue parameter N_s . Solution is Weibull modulus, m_s , 2.33; fatigue parameter, N_s , 13.1.

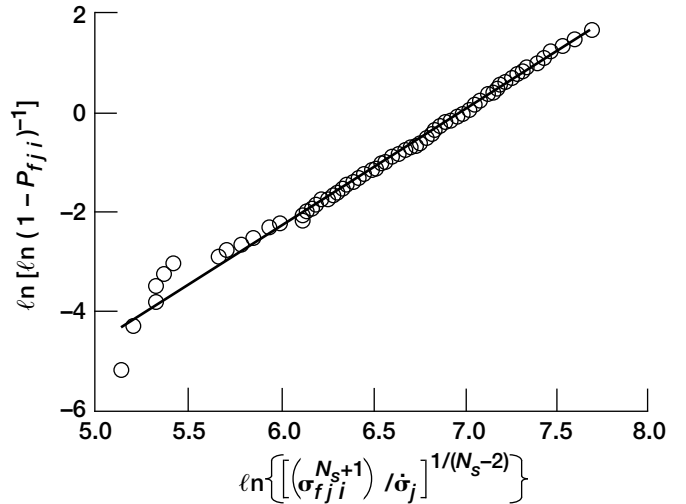


Figure 8.—Median deviation distribution for fatigue parameter, N_s , 13.1; Weibull modulus, m_s , 2.33; Z , 1083.8 $(\text{MPa}^{N_s-2} \text{sec})^{1/(N_s-2)}$. The terms P_{fji} and Z are defined in equation (70).

diagrams of the specimens, including nominal dimensions, are in figure 9. The SASC dynamic fatigue data are the mean values based on at least seven specimens. They are assumed herein to be the median values. For this material, inherent volume flaws were the source of failure (refs. 4 and 5).

Inert data analysis.—For the sintered alpha silicon carbide material, inert parameters are obtained using the least-squares best-fit and maximum likelihood estimation methods. Figures 10 to 13 show plots of the SASC O-ring and C-ring inert data and the solutions obtained using the least-squares best-fit method. Figures 14 to 17 show plots of the SASC O-ring and C-ring inert data and the solutions obtained using the maximum likelihood estimation method.

TABLE V.—INERT DATA FROM SINTERED ALPHA SILICON CARBIDE O-RING AND C-RING TEST SPECIMENS

Specimen number, j	O-ring		C-ring	
	Temperature, °C			
	1200	1300	1200	1300
	Fracture stress, σ_{fj} , MPa			
1	350.3	281.0	256.9	249.5
2	286.4	309.4	237.0	207.5
3	268.1	265.4	215.9	235.9
4	242.4	301.1	254.2	247.5
5	338.2	337.9	213.9	180.6
6	294.7	253.5	231.9	249.0
7	284.3	273.3	215.7	198.2
8	300.5	233.9	246.6	209.0
9	248.6	291.0	296.9	202.1
10	287.2	302.3	219.2	277.3
11	268.6	272.1	248.4	266.4
12	283.2	284.1	262.0	305.6
13	265.7	313.9	291.3	259.6
14	307.1	231.3	264.4	253.0
15	274.3	282.0	251.4	300.0
16	276.3	299.9	243.0	180.8
17	291.7	268.6	200.2	316.3
18	303.5	220.6	266.4	278.9
19	293.1	227.7	200.8	285.7
20	272.4	---	289.9	---

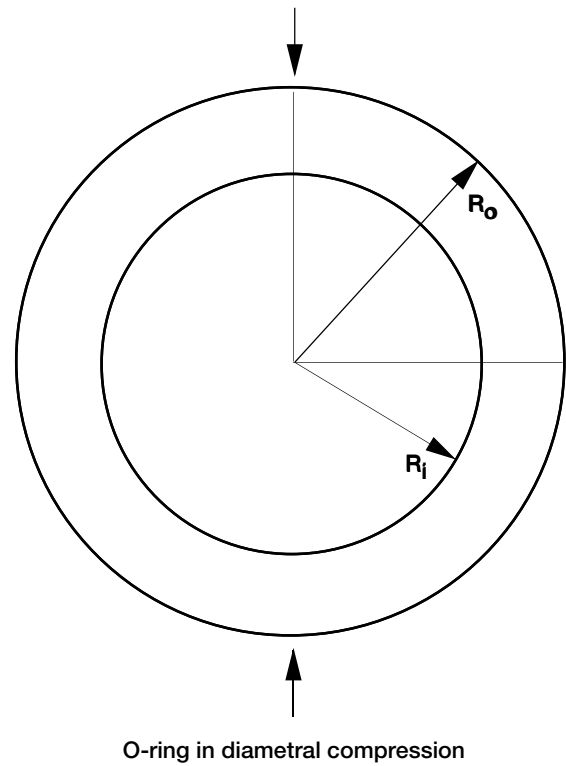
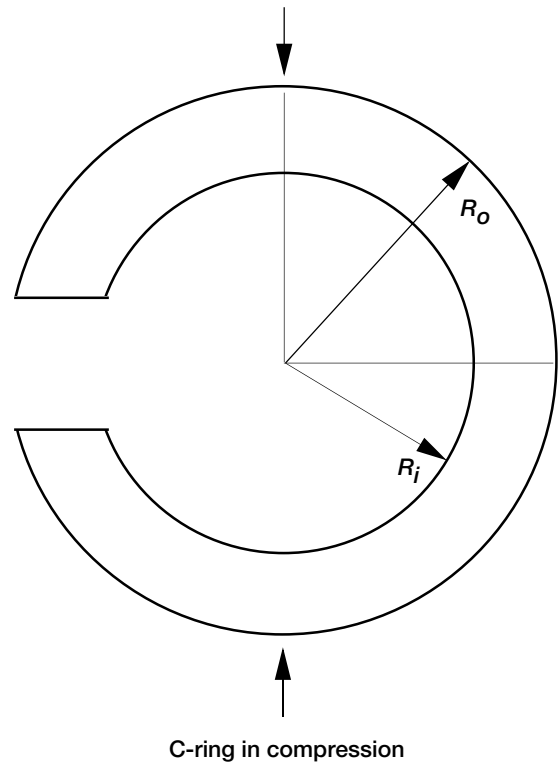


TABLE VI.—DYNAMIC FATIGUE MEDIAN VALUES FROM SINTERED ALPHA SILICON CARBIDE O-RING AND C-RING TEST SPECIMENS

Stress rate, $\dot{\sigma}_f$, MPa/sec	Temperature, °C	
	1200	1300
	Fracture stress, σ_{fj} , MPa	
O-ring		
350.0	275.7	313.5
35.0	251.2	271.7
3.5	234.2	249.8
C-ring		
100.0	253.9	256.0
10.0	229.3	225.4
1.0	218.2	205.4



Dynamic fatigue data analysis.—Table VI contains median values of SASC O-ring and C-ring dynamic fatigue test data at 1200 and 1300 °C and at three stress rates. The least-squares best-fit method is applied to the dynamic fatigue data by using the inert parameters obtained via the MLE method. Figures 18 and 19 show plots of the O-ring and C-ring dynamic fatigue data and the solutions obtained using the least-squares best-fit

Figure 9.—O-ring and C-ring test specimen configuration and nominal dimensions. Outer radius, R_o , 22.2 mm; inner radius, R_i , 17.6 mm; width, 4.6 mm.

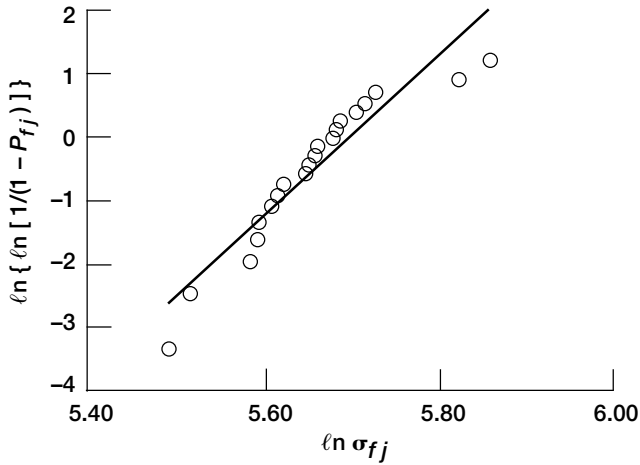


Figure 10.—Least-squares best fit to 1200 °C SASC O-ring inert data. Weibull modulus, m_V , 12.51; scale factor, σ_{OV} , 65.98 MPa-m^{3/m_V}; effective volume, V_e , 6.32 mm³.

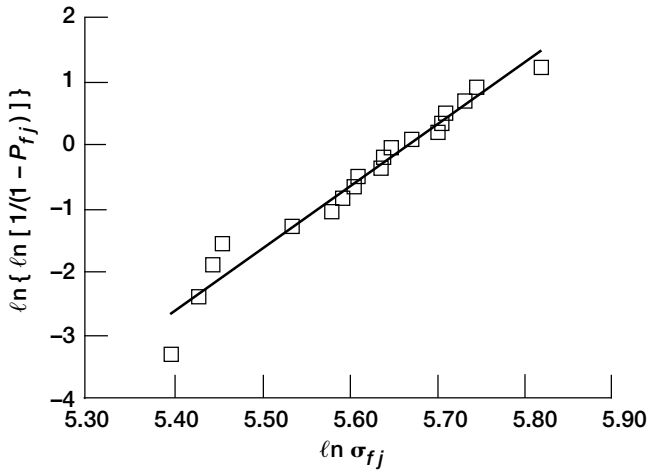


Figure 11.—Least-squares best fit to 1300 °C SASC O-ring inert data. Weibull modulus, m_V , 9.66; scale factor, σ_{OV} , 41.59 MPa-m^{3/m_V}; effective volume, V_e , 7.07 mm³.

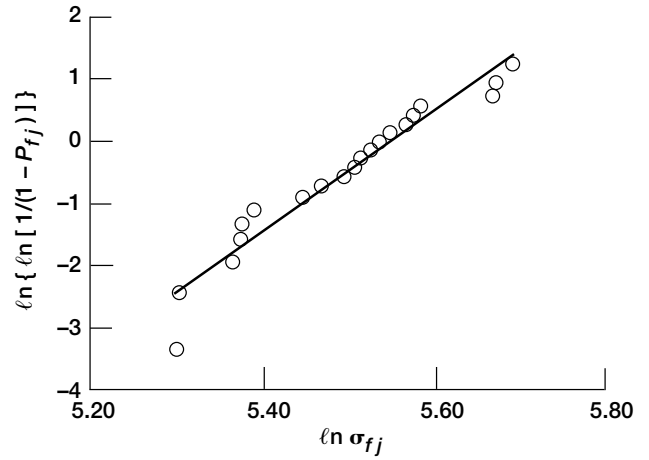


Figure 12.—Least-squares best fit to 1200 °C SASC C-ring inert data. Weibull modulus, m_V , 9.63; scale factor, σ_{OV} , 43.89 MPa-m^{3/m_V}; effective volume, V_e , 39.20 mm³.

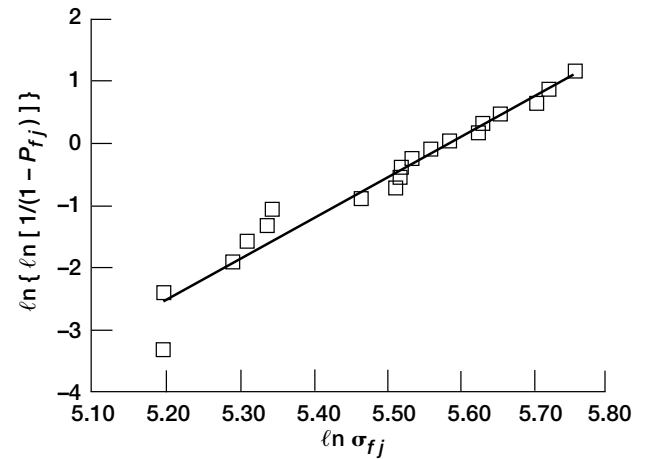


Figure 13.—Least-squares best fit to 1300 °C SASC C-ring inert data. Weibull modulus, m_V , 6.56; scale factor, σ_{OV} , 20.91 MPa-m^{3/m_V}; effective volume, V_e , 58.00 mm³.

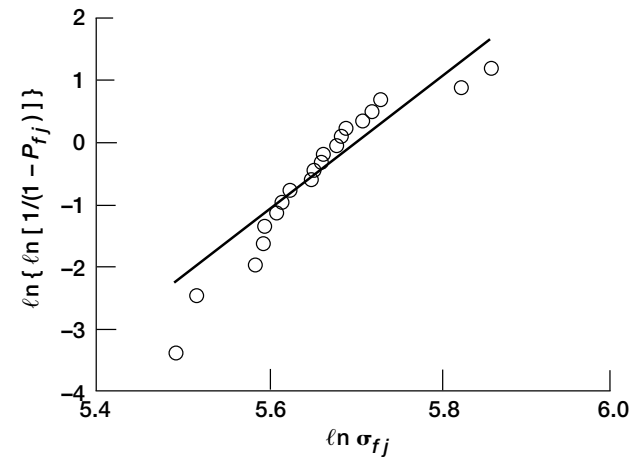


Figure 14.—Maximum likelihood estimation fit to 1200 °C SASC O-ring inert data. Weibull modulus, m_V , 10.68; scale factor, σ_{OV} , 51.02 MPa-m^{3/m_V}; effective volume, V_e , 6.32 mm³.

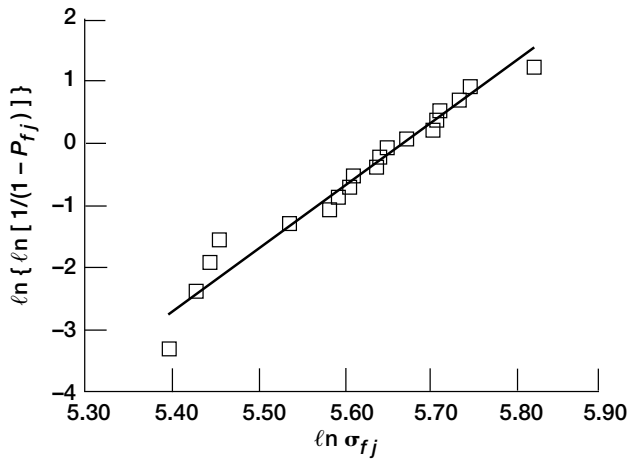


Figure 15.—Maximum likelihood estimation fit to 1300 °C SASC O-ring inert data. Weibull modulus, m_v , 10.01; scale factor, σ_{ov} , 44.49 MPa-m³/ m_v ; effective volume, V_e , 7.07 mm³

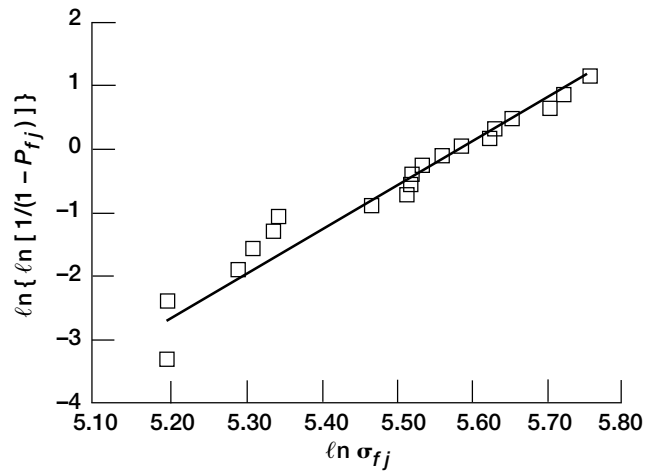


Figure 17.—Maximum likelihood estimation fit to 1300 °C SASC C-ring inert data. Weibull modulus, m_v , 7.04; scale factor, σ_{ov} , 24.82 MPa-m³/ m_v ; effective volume, V_e , 58.00 mm³.

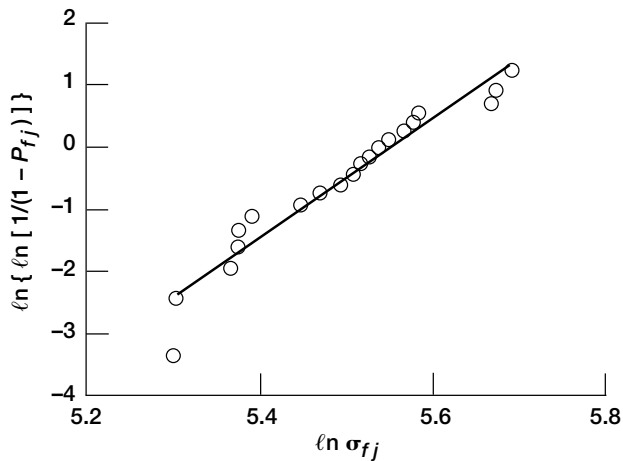


Figure 16.—Maximum likelihood estimation fit to 1200 °C SASC C-ring inert data. Weibull modulus, m_v , 9.46; scale factor, σ_{ov} , 42.52 MPa-m³/ m_v ; effective volume, V_e , 39.20 mm³.

Temperature, °C	Weibull modulus, m_v	Scale factor, σ_{ov} , MPa-m ³ / m_v	Fatigue parameters N_v	B_{WV} , MPa ² -hr
□ 1200	10.68	51.02	27.23	0.112
○ 1300	10.01	44.49	19.30	4.992

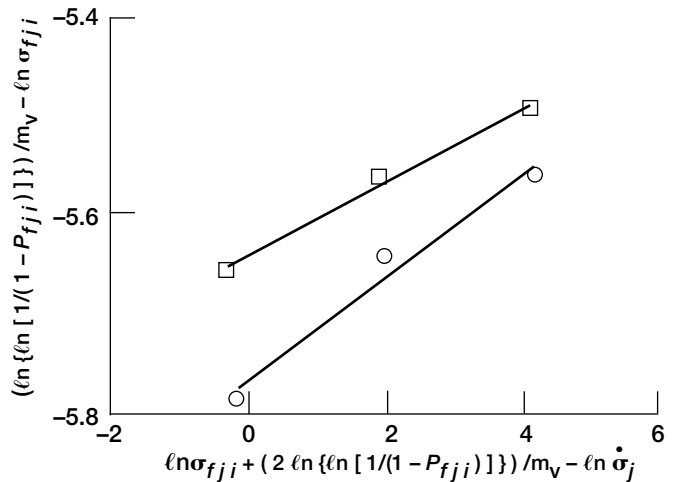


Figure 18.—Least-squares best fit to SASC O-ring dynamic fatigue median data.

Temperature, °C	Weibull modulus, m_v	Scale factor, $\sigma_{ov}, \text{MPa}\cdot\text{m}^{3/m_v}$	Fatigue parameters N_v	$B_{wv}, \text{MPa}^2\cdot\text{hr}$
□ 1200	9.46	42.52	29.43	0.461
○ 1300	7.04	24.82	19.93	0.551

method based on equation (66). The slope of the line is given by $1/N_v$. For median values, the formulation generally used is

$$\ln \sigma_{fji} = \frac{\ln \dot{\sigma}_j}{N_v + 1} + C_{ji} \quad (74)$$

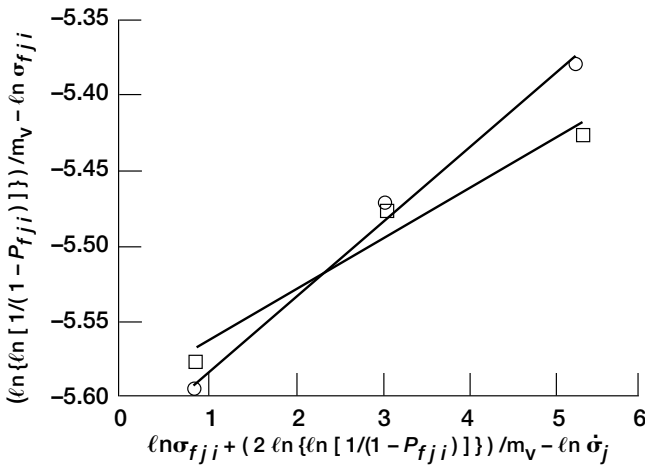


Figure 19.—Least-squares best fit to SASC C-ring dynamic fatigue median data.

where

$$\sigma_{fji} = \sigma_{fj}$$

and

$$C_{ji} = \frac{N_v - 2}{N_v + 1} \frac{\ln \left[\ln \left(\frac{1}{1 - P_{fji}} \right) \right]}{m_v} - \frac{\ln \left[\frac{V_{ef}^{(N_v - 2)/m_v}}{(N_v + 1) B_{wv} \sigma_{ov}^{N_v - 2}} \right]}{N_v + 1}$$

C_{ji} is a constant since $P_{fji} = 0.5$ for the median values. The general equation (66) was used to compute the fatigue parameters.

TABLE VII.—SUMMARY OF RESULTS FOR SODA LIME GLASS RING-ON-RING SPECIMENS

Method	Data results								
	Inert				Dynamic fatigue				
	Weibull modulus, m_s	Characteristic strength, $\sigma_{\theta s}, \text{MPa}$	Scale factor, $\sigma_{os}, \text{MPa}\cdot\text{m}^{2/m_s}$	Effective area, A_e, mm^2	Surface fatigue exponent, N_s	Weibull fatigue parameter, $B_{ws}, \text{MPa}^2\cdot\text{hr}$	Surface fatigue exponent, N_s	Weibull fatigue parameter, $B_{ws}, \text{MPa}^2\cdot\text{hr}$	Effective area, A_{ef}, mm^2
Results from present analysis									
Least-squares best fit	2.675	387.0	15.76	191.0	---	---	12.68	1.21	171.4
	2.675	387.0	15.76	191.0	13.84	0.468	---	---	173.0
Maximum likelihood	2.869	385.9	19.20	182.6	No convergence				
Median deviation	2.33	---	(a)	---	13.1	(a)	---	---	---
Results from Nemeth et al. ^b									
Least-squares best-fit median values	2.675	395.3	22.37	(b)	---	---	12.60	(b)	(b)
Maximum likelihood	2.871	394.2	---	---	---	---	---	---	---
Median deviation	2.344	---	15.00	(b)	11.88	2.29	---	---	(b)

^aThe product $(B_{ws} \sigma_{os}^{N_s - 2})$ is known from eq. (70).

^bValues based on Batdorf model in Nemeth et al.: CARES/LIFE Ceramic Analysis and Reliability Evaluation of Structures Life Prediction Program. NASA Lewis Research Center, unpublished data, 1993.

TABLE VIII.—SUMMARY OF RESULTS FOR SINTERED ALPHA SILICON CARBIDE SPECIMENS

Specimen	Temperature, °C	Least-squares best-fit inert data				Least-squares best-fit dynamic fatigue data median values		
		Weibull modulus, m_v	Characteristic strength, $\sigma_{\theta v}$, MPa	Weibull scale factor, σ_{ov}^* , MPa-m ^{3/m_v}	Effective volume V_e , mm ³	Fatigue parameters		Effective volume V_{ef} , mm ³
						N_v	B_{pvs} , MPa ² - hr	
O-ring	1200	12.51	298.5	65.98	6.32	27.24	0.11	5.38
	1300	9.66	290.3	41.59	7.07	19.30	4.98	5.77
C-ring	1200	9.63	257.9	43.89	39.20	29.43	1.61	35.60
	1300	6.56	265.2	20.91	58.00	19.92	1.96	50.50
		Maximum likelihood inert data				Least-squares best-fit dynamic fatigue data median values		
O-ring	1200	10.68	298.9	51.02	6.32	27.23	0.11	5.38
	1300	10.01	290.1	44.49	7.07	19.30	4.99	5.77
C-ring	1200	9.46	258.0	42.52	39.20	29.43	1.61	35.60
	1300	7.04	264.7	24.82	58.00	19.92	1.94	50.50

Table VII contains a summary of the inert and fatigue parameters from the analysis of the soda lime glass data. Table VIII contains a summary of the inert and fatigue parameters from the analysis of the sintered alpha silicon carbide data.

The theoretical development and experimental applications presented indicate that the general equation (66) or (73) should be applied to obtain the fatigue parameters when all the specimen rupture data are used. For the median values, equation (66) was used in preference to equation (74).

Conclusions

A reliability analysis of monolithic structural ceramics depends on material inert and fatigue parameters obtained from fast-fracture and time-dependent stress rupture data. Integrated design computer programs such as CARES/LIFE (Ceramics Analysis and Reliability Evaluation of Structures LIFE Prediction Program) use analytical methods such as those presented in this report to estimate material parameters and subsequently determine the time-dependent reliability of complex structural ceramic components.

For fast-fracture reliability analysis, specimen rupture data are utilized to determine the inert material Weibull parameters. In the examples presented, the least-squares best-fit (LSBF) and maximum likelihood estimation (MLE) methods were applied to obtain the material inert parameters for soda lime glass ring-on-ring and sintered alpha silicon carbide O-ring and C-ring specimens. Simulations have shown that the standard deviation for the MLE method is smaller than that for the LSBF method. The direct relationship of the standard deviation to the preciseness of the value calculated suggests that the MLE method is preferred. However, all experimental data reflect some degree of error as well as flaw variability. Furthermore,

the two-parameter Weibull distribution is assumed adequate and the effect of the shear stress distribution in the flexure test bar is assumed negligible. With the many apparent uncertainties, both methods (MLE and LSBF) are presumed acceptable.

For time-dependent reliability analysis, the material fatigue parameters, in addition to the inert Weibull parameters, must be evaluated. In the examples presented, dynamic fatigue data are utilized in conjunction with known inert parameters (obtained via the LSBF and/or MLE methods) to generate material fatigue parameters for the soda lime glass and SASC. Both examples included illustrate the successful use of the LSBF method to determine the fatigue parameters. However, the MLE method applied to the dynamic fatigue soda lime glass data from ring-on-ring specimens did not converge to a solution. A third approach, the median deviation method (MD), was also successfully used in conjunction with the dynamic fatigue data to obtain the cumulative distribution curve for the soda lime glass.

A comparison of results obtained for different models (Weibull and Batdorf) is given. Different models resulted in different equations for the effective area and fatigue parameters. The median deviation method was applied to the dynamic fatigue data to obtain a qualitative estimate of the Weibull modulus, exponential fatigue parameter, and the product parameter. Although these results are sufficient to define the probability distribution function of the test data, the individual values (scale factor and fatigue constant) comprising the product parameter are necessary for life prediction.

Lewis Research Center
National Aeronautics and Space Administration
Cleveland, Ohio, September 7, 1995

References

1. Wiederhorn, S.M.: Subcritical Crack Growth in Ceramics. Fracture Mechanics of Ceramics, R.C. Bradt, D.P. Hasselaur, and F.F. Lang, eds., Plenum Press, New York, 1974, pp. 613–646.
2. Paris, P.; and Erdogan, F.: A Critical Analysis of Crack Propagation Laws. J. Basic Eng. Trans. ASME, vol. 85, Dec. 1963, pp. 528–534.
3. Walker, K.: Effects of Environmental and Complex Load History on Fatigue Life. Am. Soc. Test. Mater. Spec. Tech. Publ. 462, Philadelphia, PA, 1970, p. 1.
4. Jadaan, O.M.: Fast Fracture and Lifetime Prediction of Ceramic Tubular Components. Ph.D. Thesis, Pennsylvania State Univer., 1990.
5. Jadaan, O.M.; and Tressler, R.E.: Methodology to Predict Delayed Failure Due to Slow Crack Growth in Ceramic Tubular Components Using Data From Simple Specimens. J. Eng. Mater. Technol., Trans. ASME, vol. 115, April 1993, pp. 204–210.
6. Mencik, J: Rationalized Load and Lifetime of Brittle Materials. Am. Cer. Soc. Commun., vol. 67, March 1984, pp. C–37–40.
7. Boehm, F.: A Stress-Strength Interference Approach to Fast and Delayed Fracture Reliability Analysis for Ceramic Components. Ph.D. Thesis, Northwestern University, 1989.
8. Thiemeier, T.: Lebensdauervorhersage für keramische Bauteile unter mehrachsiger Beanspruchung. Ph.D. Dissertation, Universität Karlsruhe, Germany, 1989.
9. Kapur, K.C.; and Lamberson, L.R.: Reliability in Engineering Design. John Wiley and Sons, Inc., New York, 1977.
10. Spiegel, M.R.: Schaum's Outline of Theory and Problems of Statistics. McGraw-Hill Publishing Co., New York, 1961.
11. Langlois, R.: Estimation of Weibull Parameters. J. Mater. Sci. Lett., vol. 10, 1991, pp. 1049–1051.
12. Baratta, F.L.; Quinn, G.D.; and Matthews, W.T.: Errors Associated With Flexure Testing of Brittle Materials. U.S. Army Materials Technology Laboratory, MTL–TR–87–35, July 1987.

REPORT DOCUMENTATION PAGE

Form Approved
OMB No. 0704-0188

Public reporting burden for this collection of information is estimated to average 1 hour per response, including the time for reviewing instructions, searching existing data sources, gathering and maintaining the data needed, and completing and reviewing the collection of information. Send comments regarding this burden estimate or any other aspect of this collection of information, including suggestions for reducing this burden, to Washington Headquarters Services, Directorate for Information Operations and Reports, 1215 Jefferson Davis Highway, Suite 1204, Arlington, VA 22202-4302, and to the Office of Management and Budget, Paperwork Reduction Project (0704-0188), Washington, DC 20503.

1. AGENCY USE ONLY (Leave blank)		2. REPORT DATE March 1996	3. REPORT TYPE AND DATES COVERED Technical Memorandum	
4. TITLE AND SUBTITLE Fatigue Parameter Estimation Methodology for Power and Paris Crack Growth Laws in Monolithic Ceramic Materials			5. FUNDING NUMBERS WU-505-63-5B	
6. AUTHOR(S) Bernard Gross, Lynn M. Powers, Osama M. Jadaan, and Lesley A. Janosik				
7. PERFORMING ORGANIZATION NAME(S) AND ADDRESS(ES) National Aeronautics and Space Administration Lewis Research Center Cleveland, Ohio 44135-3191			8. PERFORMING ORGANIZATION REPORT NUMBER E-9703	
9. SPONSORING/MONITORING AGENCY NAME(S) AND ADDRESS(ES) National Aeronautics and Space Administration Washington, D.C. 20546-0001			10. SPONSORING/MONITORING AGENCY REPORT NUMBER NASA TM-4699	
11. SUPPLEMENTARY NOTES Bernard Gross, Distinguished Research Associate; Lynn M. Powers, Cleveland State University, Cleveland, Ohio 44115 and NASA Resident Research Associate at Lewis Research Center; Osama M. Jadaan, University of Wisconsin-Platteville, Platteville, Wisconsin 53818 and Summer Faculty Fellow at Lewis Research Center; Lesley A. Janosik, NASA Lewis Research Center. Responsible person, Lesley A. Janosik, organization code 5250, (216) 433-5160.				
12a. DISTRIBUTION/AVAILABILITY STATEMENT Unclassified - Unlimited Subject Category 39 This publication is available from the NASA Center for Aerospace Information, (301) 621-0390.			12b. DISTRIBUTION CODE	
13. ABSTRACT (Maximum 200 words) Material parameters (inert and fatigue) are obtained from naturally flawed specimens. If the inert strength parameters characterizing the two-parameter Weibull cumulative distribution function are known, the fatigue parameters for the power, Paris, and Walker subcritical crack growth equations can be obtained from the appropriate rupture data of standard uniaxial test specimens loaded in static, dynamic, or cyclic fatigue. Equations are developed for fatigue parameter analysis using the least-squares best-fit and/or the maximum likelihood estimation method. When the inert parameters are unknown and only subcritical crack growth rupture data are available, the material parameters defining the specimen's cumulative distribution function are obtained via the median deviation method. Example problems are included.				
14. SUBJECT TERMS Monolithic ceramics; Parameter estimation; Weibull distribution; Reliability; Life prediction			15. NUMBER OF PAGES 28	
			16. PRICE CODE A03	
17. SECURITY CLASSIFICATION OF REPORT Unclassified	18. SECURITY CLASSIFICATION OF THIS PAGE Unclassified	19. SECURITY CLASSIFICATION OF ABSTRACT Unclassified	20. LIMITATION OF ABSTRACT	